

BCSJ Award Article

Kinetically Stabilized 1,1′-Bis[(*E*)-diphosphenyl]ferrocenes: Syntheses, Structures, Properties, and Reactivity#

Noriyoshi Nagahora,[1,2] Takahiro Sasamori,[1] Yasuaki Watanabe,[3] Yukio Furukawa,[3] and Norihiro Tokitoh*[1]

[1]Institute for Chemical Research, Kyoto University, Gokasho, Uji, Kyoto 611-0011

[2]Institute of Sustainability Science, Kyoto University, Gokasho, Uji, Kyoto 611-0011

[3]Department of Chemistry, School of Science and Engineering, Waseda University, 3-4-1 Okubo, Shinjuku-ku, Tokyo 169-8555

Received May 2, 2007; E-mail: tokitoh@boc.kuicr.kyoto-u.ac.jp

Kinetically stabilized 1,1′-bis[(*E*)-diphosphenyl]ferrocenes were synthesized by taking advantage of extremely bulky substituents, 2,4,6-tris[bis(trimethylsilyl)methyl]phenyl (denoted as Tbt) and 2,6-bis[bis(trimethylsilyl)methyl]-4-[tris(trimethylsilyl)methyl]phenyl (denoted as Bbt) groups, and characterized by the spectroscopic and X-ray crystallographic analyses. The electronic structures of the 1,1′-bis[(*E*)-diphosphenyl]ferrocenes were determined by analyzing electronic spectra, the transitions of which were reasonably assigned based on theoretical calculations. In the cyclic voltammograms, there were two well-defined reversible one-electron reduction couples corresponding to the intramolecular two diphosphene units. Furthermore, the 1,1′-bis[(*E*)-diphosphenyl]ferrocene was found to undergo ligand-exchange reactions with group 6 metal carbonyl complexes along with the *E*-to-*Z* isomerization of the diphosphene moieties, leading to the formation of the corresponding 1,1′-bis[(*Z*)-diphosphenyl]ferrocene group 6 metal tetracarbonyl complexes, $[M(CO)_4\{(Z,Z)\text{-}(BbtP{=}PC_5H_4)_2Fe\}]$ (M = Cr, Mo, and W). The molecular structures of these complexes were determined by spectroscopic analyses (^{1}H, ^{13}C, and ^{31}P NMR spectra, and UV–vis spectra), and that of the tungsten complex was determined by X-ray crystallographic analysis. Several types of d → $\pi^*_{P=P}$ electron transitions due to the iron and group 6 metals were detected by using UV–vis spectroscopy, and these results were supported by theoretical calculations.

The chemistry of heavier congeners of azo-compound (–N=N–) has been studied extensively for more than 25 years,[1] since the pioneering synthesis and isolation of the first stable diphosphene bearing 2,4,6-tri-*tert*-butylphenyl groups (Mes*P=PMes*), reported by Yoshifuji and co-workers.[2] Nowadays, it is well-known that diphosphenes, which have relatively low-lying π^* orbitals, readily undergo one-electron reduction to give their anion-radical species.[3] We have reported the synthesis of novel doubly bonded systems between heavier group 15 elements (dipnictenes), that is, diphosphene, distibene (–Sb=Sb–), dibismuthene (–Bi=Bi–), phosphabismuthene (–P=Bi–), and stibabismuthene (–Sb=Bi–), by taking advantage of bulky protecting groups, such as 2,4,6-tris[bis(trimethylsilyl)methyl]phenyl (Tbt) and 2,6-bis[bis(trimethylsilyl)methyl]-4-[tris(trimethylsilyl)methyl]phenyl (Bbt) groups (Fig. 1).[4] Furthermore, the redox properties of (*E*)-BbtE=EBbt (E = P, Sb, and Bi) have been systematically elucidated based on cyclic voltammetry and DFT calculations, and the solid-state structure of the first stable anion radical species of (*E*)-BbtSb=SbBbt has also been reported.[4i,4k]

Low-coordinated species of heavier group 15 elements have attracted much interest due to their low-lying π^* levels compared with diazenes (–N=N–) from two reasons: (i) their electrochemical properties[3] and (ii) coordination ability toward transition metals.[1a,5] Recently, unique π-conjugated systems containing diphosphene unit(s) have been developed from the former viewpoint (i). For example, a unique d(Fe)–π(P=P) electron system, (*E*)-ferrocenyldiphosphene [(*E*)-FcP=PMes* (Fc = $C_5H_4FeC_5H_5$)], has been synthesized by Niecke and Pietschnig for the first time (Fig. 2), and its absorption band

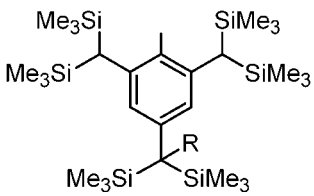

Fig. 1. Effective steric protection groups.

Published on the web October 12, 2007; doi:10.1246/bcsj.80.1884

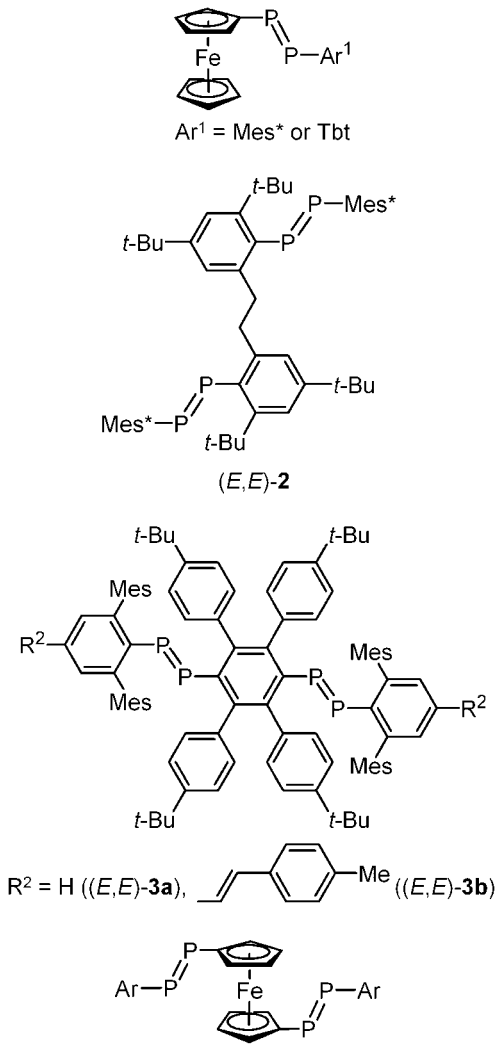

Fig. 2.

corresponding to the electron transitions from d(Fe) to π^*(P=P) orbitals has been reported.[6] However, it readily undergoes dimerization above −40 °C under daylight leading to the formation of the corresponding cyclotetraphosphane.[6] Later on, we have determined the crystal structure of a kinetically stabilized (*E*)-ferrocenyldiphosphene bearing a Tbt group and its unique electrochemical behavior.[4h] On the other hand, Protasiewicz and co-workers have synthesized 1,4-bis[(*E*)-diphosphenyl]benzene derivatives (Fig. 2), in which the P=P π electron systems are extended onto those of the conjugated aromatic rings, and they have reported unique electrochemical behavior for these π-conjugated diphosphenes.[7] We have also reported the synthesis of stable 1,1′-bis[(*E*)-diphosphenyl]ferrocenes, which have unique d–π electron systems, by utilizing Tbt ((*E*,*E*)-**1a**) and Bbt ((*E*,*E*)-**1b**) groups, and determined their crystal structures and electrochemical properties (Fig. 2).[8] Independently, Pietschnig and co-workers have reported the synthesis of (*E*,*E*)-**1a** and the stable 1,1′-bis[(*E*)-diphosphenyl]ferrocene bearing 2,6-dimesitylphenyl groups ((*E*,*E*)-**1c**).[9]

From viewpoint (ii), the chemistry of bidentate ligands bearing low-coordinated phosphorus atoms, such as 2,2′-biphosphorins[10] and 3,4-bis(diphosphinidene)cyclobutenes (DPCBs),[11] has attracted great attention in recent years due to their unique structures and strong π-acceptor abilities (Fig. 3). Meanwhile, a diphosphene moiety is well-known to work as a ligand for group 6 metals in several fashions of coordination, that is, η^1 (end-on), η^2 (side-on), $\mu_2(\eta^1{:}\eta^1)$ (end-on and end-on), $\mu_2(\eta^1{:}\eta^2)$ (end-on and side-on), and $\mu_3(\eta^1{:}\eta^1{:}\eta^2)$ (end-on, end-on, and side-on) types, using its lone-pair electrons or π orbitals as the coordination site (Fig. 4).[1a,5] From the viewpoints of both (i) electrochemical properties and (ii) coordination ability toward transition metals, 1,1′-bis[(*E*)-diphosphenyl]ferrocenes should show attractive electrochemical behavior and be a good candidate as a bidentate ligand in consideration of rotational flexibility of the cyclopentadienyl ring in a ferrocene. In this paper, we report the syntheses, structural characterization, and properties of the first 1,1′-bis[(*E*)-diphosphenyl]ferrocenes (*E*,*E*)-**1a** and (*E*,*E*)-**1b** kinetically stabilized by the Tbt and Bbt groups, respectively, and the ligand-exchange reactions of (*E*,*E*)-**1b** with group 6 metal carbonyl complexes along with unique *E*-to-*Z* isomerization of the diphosphene moieties.

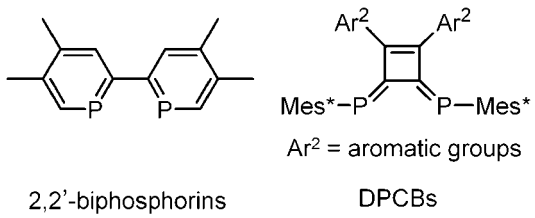

Fig. 3.

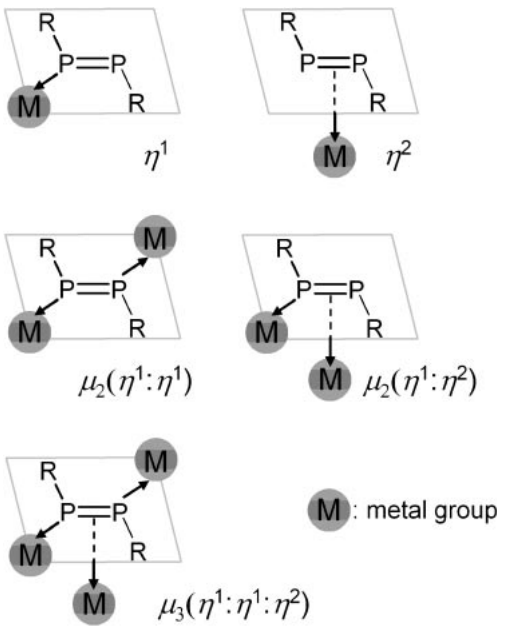

Fig. 4. Possible structures of metal complexes for diphosphene.

Results and Discussion

Syntheses of Kinetically Stabilized 1,1′-Bis[(*E*)-diphosphenyl]ferrocenes. Synthetic route for the 1,1′-bis[(*E*)-diphosphenyl]ferrocenes, (*E*,*E*)-**1a** and (*E*,*E*)-**1b**, is shown in Scheme 1. Phosphines **4a** and **4b** having Tbt and Bbt groups,

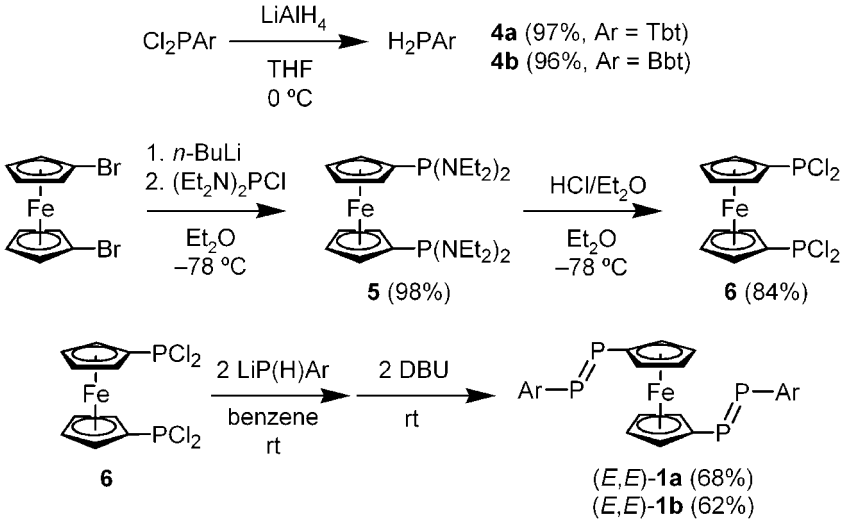

Scheme 1. Syntheses of (*E*,*E*)-**1a** and (*E*,*E*)-**1b**.

respectively, were prepared by the reaction of the corresponding dichlorophosphines with lithium aluminum hydride in excellent yields. 1,1′-Bis[bis(diethylamino)phosphino]ferrocene (**5**) was quantitatively synthesized by the reaction of bis(diethylamino)chlorophosphine with 1,1′-dilithioferrocene prepared from 1,1′-dibromoferrocene. The reaction of **5** with hydrogen chloride in ether followed by the removal of inorganic salts gave 1,1′-bis(dichlorophosphino)ferrocene (**6**) in good yield. The treatment of **6** with two molar amounts of LiP(H)Ar (Ar = Tbt (**7a**) or Bbt (**7b**)), which was prepared by the reaction of H_2PAr (Ar = Tbt (**4a**) or Bbt (**4b**)) with an equimolar amount of butyllithium in ether at −40 °C, in benzene at room temperature gave the corresponding chlorohydrodiphosphane derivatives as diastereomixtures. Subsequently, the double-dehydrochlorination reaction using 1,8-diazabicyclo[5.4.0]-undec-7-ene (DBU) at room temperature afforded 1,1′-bis[(*E*)-diphosphenyl]ferrocenes, (*E*,*E*)-**1a** and (*E*,*E*)-**1b** in >90% yields.[12] Recrystallization from their hexane solution at −40 °C gave purple powder of pure (*E*,*E*)-**1a** and (*E*,*E*)-**1b**, suitable for chemical analyses, in 68% and 62% isolated yields, respectively. Both (*E*,*E*)-**1a** and (*E*,*E*)-**1b** were thermally stable either up to 260 °C in the solid state or up to 120 °C in toluene-d_8 solution in a degassed and sealed tube. Upon exposure to daylight, neither decomposition nor isomerization of the diphosphene moieties of (*E*,*E*)-**1a** and (*E*,*E*)-**1b** was observed in the benzene-d_6 solution.

NMR Spectra of the 1,1′-Bis[(*E*)-diphosphenyl]ferrocenes, (*E*,*E*)-1a and (*E*,*E*)-1b. The molecular structures of (*E*,*E*)-**1a** and (*E*,*E*)-**1b** in solution were evaluated by their NMR spectra. The ^{1}H NMR spectra of (*E*,*E*)-**1a** and (*E*,*E*)-**1b** in benzene-d_6 exhibited one set of A_2B_2 systems with $^1J_{HH}$ = 1.8 Hz (both (*E*,*E*)-**1a** and (*E*,*E*)-**1b**) at 4.58 and 4.96 ppm (for (*E*,*E*)-**1a**) and 4.58 and 4.93 ppm (for (*E*,*E*)-**1b**), which were assigned to the protons of the cyclopentadienyl ring. The peaks indicate that the fast rotation of the C(Cp ring)–P bonds occurs at room temperature. The ^{31}P NMR spectra of (*E*,*E*)-**1a** and (*E*,*E*)-**1b** in benzene-d_6 showed a diagnostic pair of doublets at 497.3 and 488.9 ppm ((*E*,*E*)-**1a**) and 496.9 and 491.1 ppm ((*E*,*E*)-**1b**), respectively, with $^1J_{PP}$ = 550 Hz (both (*E*,*E*)-**1a** and (*E*,*E*)-**1b**), which are characteristic of (*E*)-diphosphenes

Table 1. ^{31}P NMR Data of Bis[(*E*)-diphosphene] Derivatives

	δ_P/ppm	$^1J_{PP}$/Hz	Ref.
(*E*,*E*)-**1a**[a)]	488.9, 497.3	550	this work
(*E*,*E*)-**1b**[a)]	491.1, 496.9	550	this work
(*E*,*E*)-**1c**[a)]	444.9, 470.3	537	9
(*E*,*E*)-**2**[b)]	476.7, 515.9	582.8	13
(*E*,*E*)-**3a**[b)]	481.7, 525.5	576	7a
(*E*,*E*)-**3b**[b)]	479.7, 524.8	570	7c

a) In C_6D_6. b) In $CDCl_3$.

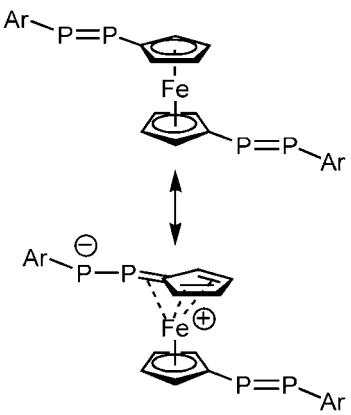

Fig. 5. Conceivable resonance structures for 1,1′-bis[(*E*)-diphosphenyl]ferrocenes.

bearing two different substituents. The ^{31}P NMR spectral data are summarized in Table 1 together with those of the previously reported bis[(*E*)-diphosphene] derivatives.[7–9,13] The observed coupling constants of (*E*,*E*)-**1a** and (*E*,*E*)-**1b** were somewhat smaller than those of the reported (*E*)-diphosphenes having two different bulky aryl groups,[1a] indicating their characteristic polarized resonance structures similar to the case of the reported (*E*)-ferrocenyldiphosphenes (Fig. 5).[4h,6] The ^{31}P NMR spectral data of several (*E*)-diphosphenes and (*E*)-ferrocenyldiphosphenes are shown in Table 2 as references.

Crystal Structures of the 1,1′-Bis[(*E*)-diphosphenyl]fer-

rocenes, (*E,E*)-1a and (*E,E*)-1b. Single crystals of (*E*,*E*)-**1a** and (*E*,*E*)-**1b** suitable for X-ray diffraction study were obtained from their benzene solutions in a degassed and sealed tube. The molecular structures of (*E*,*E*)-**1a** and (*E*,*E*)-**1b** were determined by the X-ray crystallographic analyses (Fig. 6), and their selected structural parameters are summarized in Table 3. The conformations of (*E*,*E*)-**1a** and (*E*,*E*)-**1b** in the solid states are curiously different from each other in spite of the similarity between Tbt and Bbt groups. That is, (*E*,*E*)-**1a** (triclinic, $P\bar{1}$) has a crystallographic center of symmetry at the central Fe atom, whereas (*E*,*E*)-**1b** (monoclinic, $C2/c$) has a two-fold rotation axis through the Fe atom. The torsion angle between the centroid(Cp)–P(2) moieties of (*E*,*E*)-**1b** (θ in the Fig. 6c) is 48.0°, whereas that of (*E*,*E*)-**1a** is inherently 180°. Both (*E*,*E*)-**1a** and (*E*,*E*)-**1b** has an (*E*)-conformation of the diphosphene moieties with the C–P–P–C torsion angles of 179.3(4) and 176.0(2)°, respectively, and their C–P–P–C planes are almost coplanar with the adjacent Cp ring, suggesting a conjugative interaction between the π-electrons of

Table 2. ^{31}P NMR Data of (*E*)-Diphosphenes

R	δ_P/ppm	$^1J_{PP}$/Hz
	Diphosphenes, Mes*P=PR	
Tsi[a)]	530.0, 533.1	620
Mes[b)]	467.6, 540.4	574
Tip[c)]	470, 535	572
Ph	455.5, 525.5	548
	Ferrocenyldiphosphenes, FcP=PR	
Mes*	442.6, 471.2	532
Tbt	479.5, 501.7	546

a) Tsi; tris(trimethylsilyl)methyl. b) Mes; 2,4,6-trimethylphenyl. c) Tip; 2,4,6-triisopropylphenyl.

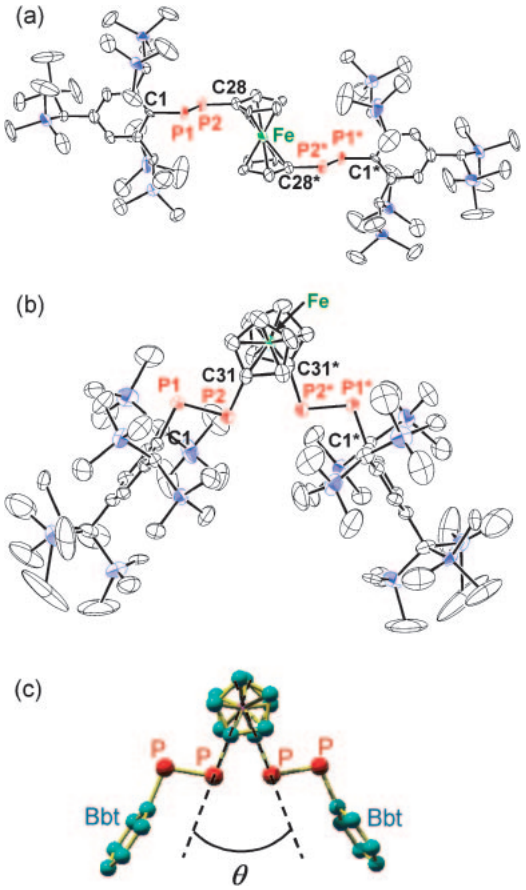

Fig. 6. ORTEP drawings of the major parts of (a) (*E*,*E*)-**1a** and (b) (*E*,*E*)-**1b** with thermal ellipsoid plots (50% probability). Hydrogen atoms are omitted for clarity. (c) Molecular structure of (*E*,*E*)-**1b** without the $CH(SiMe_3)_2$ and $C(SiMe_3)_3$ groups and hydrogen atoms.

Table 3. Observed and Calculated Structural Parameters for 1,1′-Bis[(*E*)-diphosphenyl]ferrocenes

Bond lengths/Å		Bond angles/deg		Torsion angles/deg	
		1,1′-Bis[(*E*)-diphosphenyl]ferrocene (*E*,*E*)-**1a**			
P(1)–P(2)	2.015(3)	C(1)–P(1)–P(2)	98.5(2)	C(1)–P(1)–P(2)–C(28)	−179.3(4)
P(1)–C(1)	1.860(4)	C(28)–P(2)–P(1)	102.1(5)		
P(2)–C(28)	1.797(9)				
		1,1′-Bis[(*E*)-diphosphenyl]ferrocene (*E*,*E*)-**1b**			
P(1)–P(2)	2.0398(18)	C(1)–P(1)–P(2)	103.25(15)	C(1)–P(1)–P(2)–C(31)	−176.0(2)
P(1)–C(1)	1.854(4)	C(31)–P(2)–P(1)	101.9(3)		
P(2)–C(31)	1.807(6)				
		(*E*,*E*)-**8a**			
P–P	2.055	C(Dmp)–P–P	99.8	C(Dmp)–P–P–C(Cp)	−179.2
P–C(Dmp)	1.860	C(Cp)–P–P	102.9		
P–C(Cp)	1.819				
		(*E*,*E*)-**8b**			
P–P	2.054	C(Dmp)–P–P	99.7	C(Dmp)–P–P–C(Cp)	−179.1
P–C(Dmp)	1.860	C(Cp)–P–P	103.1		
P–C(Cp)	1.822				

Table 4. Reported Raman Shifts for (*E*)-Diphosphenes ($R^1P{=}PR^2$)

R^1, R^2	ν(P=P)/cm^{-1}	Ref.
Mes*, Mes*	610	15
Tbt, Tbt	609	4f
Bbt, Bbt	603	4f
Fc, Tbt	609	4h

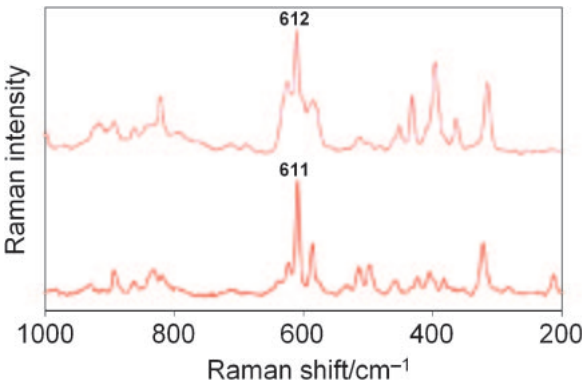

Fig. 7. Raman spectra of (top) (*E*,*E*)-**1a** and (bottom) (*E*,*E*)-**1b** using He-Ne laser (532 nm) in the solid state.

Table 5. Observed and Calculated Vibrational Spectroscopic Data for 1,1′-Bis[(*E*)-diphosphenyl]ferrocenes

	Raman, ν(P=P)/cm^{-1}	Infrared, ν(P=P)/cm^{-1}
(*E*,*E*)-**1a**, obsd[a)]	612	614
(*E*,*E*)-**1b**, obsd[a)]	611	615
(*E*,*E*)-**8a**, calcd[b)]	624	622
(*E*,*E*)-**8b**, calcd[b)]	624	624

a) Measured with the excitation by He-Ne laser (532 nm). b) Calculated at B3LYP/6-31G(d) level.

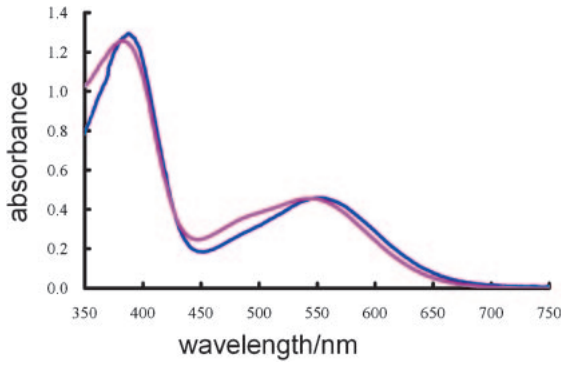

Fig. 8. UV–vis spectra of (*E*,*E*)-**1a** (purple line) and (*E*,*E*)-**1b** (blue line) in benzene.

Table 6. UV–Vis Spectral Data for 1,1′-Bis[(*E*)-diphosphenyl]ferrocenes (*E*,*E*)-**1a**, (*E*,*E*)-**1b**, and (*E*,*E*)-**1c** and 1,4-Bis[(*E*)-diphosphenyl]benzenes (*E*,*E*)-**3a** and (*E*,*E*)-**3b**

	$\lambda_1(\pi{-}\pi^*)$/nm	λ_2(n–π^*)/nm	λ_3(d–π^*)/nm	Ref.
(*E*,*E*)-**1a**[a)]	384 (ε 7300)	480 (ε 1800)	539 (ε 2200)	this work
(*E*,*E*)-**1b**[a)]	389 (ε 7400)	485 (ε 1300)	553 (ε 2200)	this work
(*E*,*E*)-**1c**[a)]	351[d)]	—[e)]	542[d)]	9
(*E*,*E*)-**3a**[b)]	390 (ε 7550)	476 (ε 870)	—	7a
(*E*,*E*)-**3b**[c)]	422 (ε 19000)	481 (ε 2100)	—	7c

a) In benzene. b) In hexane. c) In chloroform. d) The molar absorptivity was not presented. e) The wavenumber of the absorption maximum was not mentioned.

the diphosphene units with those of the Cp rings of (*E*,*E*)-**1a** and (*E*,*E*)-**1b**. Their P=P bond lengths (2.015(3) Å for (*E*,*E*)-**1a** and 2.0398(18) Å for (*E*,*E*)-**1b**) are considerably shorter than the typical P–P single-bond lengths (ca. 2.19–2.24 Å)[14] and are within the range of those found for the previously reported (*E*)-diaryldiphosphenes (1.985–2.049 Å).[1a,4f] Moreover, the P–P–C bond angles of (*E*,*E*)-**1a** and (*E*,*E*)-**1b** are 98.5(2) and 102.1(5)° for (*E*,*E*)-**1a** and 103.25(15) and 101.9(3)° for (*E*,*E*)-**1b**, respectively, and are within the range of those for previously reported (*E*)-diaryldiphosphenes (97.8(1)–114.9(1)°).[2,4f,4l] These results strongly indicated the P=P double-bond character of (*E*,*E*)-**1a** and (*E*,*E*)-**1b** in the solid state.

Raman and Infrared Spectra of 1,1′-Bis[(*E*)-diphosphenyl]ferrocenes. Raman spectroscopy is a valuable tool to evaluate the double-bond character of diphosphenes in the solid sate.[1c,4f,15] It is known that their intense Raman shifts corresponding to the P=P stretching for the reported (*E*)-diphosphene compounds are in the range from 603 to 610 cm^{-1} (Table 4),[1c,4f,4l,15] while that of the diphosphane Ph_2P–PPh_2 appeared at 530 cm^{-1}.[16] The Raman spectra of (*E*,*E*)-**1a**/(*E*,*E*)-**1b** were measured in the solid state with 532 nm excitation in a degassed and sealed tube. In Fig. 7, the Raman spectra of (*E*,*E*)-**1a**/(*E*,*E*)-**1b** are shown, and the most intense signals were at 612/611 cm^{-1}, respectively, which were similar to those of the (*E*)-diaryldiphosphenes[4f,15] and (*E*)-ferrocenyldiphosphene (Tables 4 and 5).[4h] Interestingly, the Infrared spectra of (*E*,*E*)-**1a**/(*E*,*E*)-**1b** in the solid state (KBr disks) showed the characteristic signals for P=P at 614/615 cm^{-1}, respectively. The characteristic P=P vibrational frequencies of (*E*,*E*)-**1a**/(*E*,*E*)-**1b** were found to be active for both Raman (ν = 612/611 cm^{-1}) and IR (ν = 614/615 cm^{-1}) spectroscopy in the solid state due to the symmetric and asymmetric stretching modes, the assignment of which was supported by theoretical calculations on the model molecules (*E*,*E*)-**8a**/(*E*,*E*)-**8b** (vide infra).

UV–Vis Spectra of 1,1′-Bis[(*E*)-diphosphenyl]ferrocenes. The UV–vis spectra of (*E*,*E*)-**1a**/(*E*,*E*)-**1b** in benzene showed three absorption maxima at 384/389 (ε = 7300/7400), 480/485 (sh, ε = 1800/1300), and 539/553 nm (ε = 2200/2200) as shown in Fig. 8. The data are summarized in Table 6.

The first one ($\lambda_{max} = 384/389$ nm), which was assigned to the $\pi \rightarrow \pi^*$ electron transitions based on the large ε, was within the range of those reported for (*E*)-diaryldiphosphenes (277–418 nm),[1a,4f] showing a hypsochromic shift similar to those for the 1,4-bis[(*E*)-diphosphenyl]benzenes (*E*,*E*)-**3a**/(*E*,*E*)-**3b** (398/422 nm) reported by Protasiewicz's group.[7] The second one ($\lambda_{max} = 480/485$ nm) was assigned to the $n \rightarrow \pi^*$ electron transitions for the diphosphene units, based on previous reports of those for the (*E*)-diaryldiphosphenes (437–532 nm)[1a,4f] and (*E*,*E*)-**3a**/(*E*,*E*)-**3b** (476/481 nm).[7] The third one ($\lambda_{max} = 539/553$ nm) was attributed to the metal-to-ligand charge-transfer transitions (MLCT band) due to the electron transitions from d orbitals of the iron atom to the π^* orbital of the P=P moiety, where a subtle bathochromic shift was observed as compared with those for (*E*)-FcP=PAr (Ar = Mes*; 515 nm,[6] Ar = Tbt; 542 nm[4h]). In addition, the assignment of the observed absorption maxima for (*E*,*E*)-**1a**/(*E*,*E*)-**1b** was reasonably supported by theoretical calculations for the excited states of their model molecules (vide infra).

Theoretical Calculations for 1,1′-Bis[(*E*)-diphosphenyl]-ferrocenes. In order to understand the electronic structures of 1,1′-bis[(*E*)-diphosphenyl]ferrocenes, we performed theoretical calculations for the model molecules, where the Tbt and Bbt groups of (*E*,*E*)-**1a** and (*E*,*E*)-**1b**, respectively, were replaced by 2,6-dimethylphenyl (denoted as Dmp) groups. In the structural optimization of the model molecule [Fe(C_5H_4P=PDmp)$_2$] by using B3LYP at 6-31G(d) level, two local minima, which were named as (*E*,*E*)-**8a** and (*E*,*E*)-**8b**, were found as geometries similar to the solid-state structures of (*E*,*E*)-**1a** and (*E*,*E*)-**1b**, respectively. The selected structural parameters and full theoretically optimized coordinates of (*E*,*E*)-**8a** and (*E*,*E*)-**8b** are shown in Table 3 and the Supporting Information (Tables S1 and S2), respectively. It was found that the SCF energy of (*E*,*E*)-**8a** was smaller than that of (*E*,*E*)-**8b** by only 1.2 kJ mol^{-1}, indicating the difference in the crystalline geometries observed for (*E*,*E*)-**1a** and (*E*,*E*)-**1b** should be due to the packing force. Theoretical calculations for the vibrational frequencies of (*E*,*E*)-**8a** and (*E*,*E*)-**8b** showed the two characteristic stretching vibrations for the P=P double-bonds arising from the phase of the two intramolecular diphosphene units, respectively. Namely, it was found that the symmetric and asymmetric stretching vibrations for (*E*,*E*)-**8a**/(*E*,*E*)-**8b** appeared at 624/624 and 622/624 cm^{-1}, respectively (Fig. 9 and Table 5). The former should be Raman active (624 nm for (*E*,*E*)-**8a** and 622 nm for (*E*,*E*)-**8b**), whereas the latter is Infrared active (624 nm for both (*E*,*E*)-**8a** and (*E*,*E*)-**8b**). These calculated results are in good agreement with those obtained from the Raman and IR spectra of (*E*,*E*)-**1a** and (*E*,*E*)-**1b**. In addition, calculations on the excited states of (*E*,*E*)-**8a** and (*E*,*E*)-**8b** were also performed by using TDDFT. The results are shown in Table S3 (Supporting Information) together with the UV–vis spectral data of (*E*,*E*)-**1a** and (*E*,*E*)-**1b**. Calculations on (*E*,*E*)-**8a** and (*E*,*E*)-**8b** at B3LYP/TZ(2d) for Fe, 6-311+G(2d) for P, and 6-31G(d) for C, H level showed that the low-lying excitation energy for (*E*,*E*)-**8a** and (*E*,*E*)-**8b** predominantly corresponded to $d_{Fe} \rightarrow \pi^*_{P=P}$ transitions. Thus, the low-lying vacant orbitals (LUMO and LUMO+1) for (*E*,*E*)-**8a** and (*E*,*E*)-**8b** have $\pi^*_{P=P}$ character, whereas the HOMO orbital is localized on d orbitals of the iron atom (Fig. 10). Transitions from the $n_{P=P}$ (HOMO−3 and HOMO−4) to the $\pi^*_{P=P}$ orbitals were estimated to be at 457.3 nm for (*E*,*E*)-**8a** and 463.6 nm for (*E*,*E*)-**8b**. Moreover, it was predicted that the high-energy region of singlet excitations of (*E*,*E*)-**8a** and (*E*,*E*)-**8b** in the gas phase were the allowed $\pi_{P=P} \rightarrow \pi^*_{P=P}$ transitions, which are in agreement with the experimental results. Consequently, the assignment of the observed UV–vis spectra of (*E*,*E*)-**1a** and (*E*,*E*)-**1b** were reasonably supported by the TDDFT calculations for the model molecule [Fe(C_5H_4P=PDmp)$_2$].

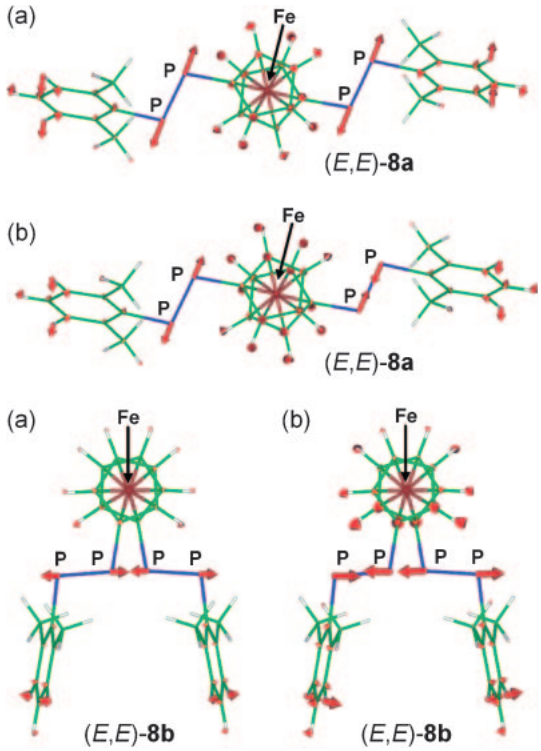

Fig. 9. Schematic eigenvectors for the selected intense (a) Raman-active symmetric and (b) infrared-active asymmetric vibrations of (*E*,*E*)-**8a** and (*E*,*E*)-**8b** calculated at the B3LYP/6-31G(d) level.

Electrochemical Properties of 1,1′-Bis[(*E*)-diphosphenyl]ferrocenes. There have been a number of reports on the electrochemical properties of diphosphenes, showing reversible one-electron reduction couples for (*E*)-diphosphenes observed by cyclic voltammetry.[3,4g–i,4k,4l,8] The redox behavior of (*E*,*E*)-**1a** and (*E*,*E*)-**1b** was also analyzed by cyclic and differential pulse voltammetries, and the voltammograms are shown in Fig. 11. The observed redox potentials and the resulting comproportionation constants of (*E*,*E*)-**1a** and (*E*,*E*)-**1b** are summarized in Table 7. In the THF solution, two reversible one-electron redox waves due to the stepwise reduction of the intramolecular two redox centers were observed at −1.84 and −2.19 V ((*E*,*E*)-**1a**) and −1.78 and −2.13 V ((*E*,*E*)-**1b**) versus Ag/Ag$^+$, respectively. The first reduction potentials of (*E*,*E*)-**1a** and (*E*,*E*)-**1b** were similar to those of the reported (*E*)-diphosphenes under similar conditions.[3,4g–i,4k,4l,8] For both (*E*,*E*)-**1a** and (*E*,*E*)-**1b**, the difference between the half-potentials ($\Delta E_{1/2} = 0.35$ V), which is commonly used as a guide to an extent of electronic interaction between the two-

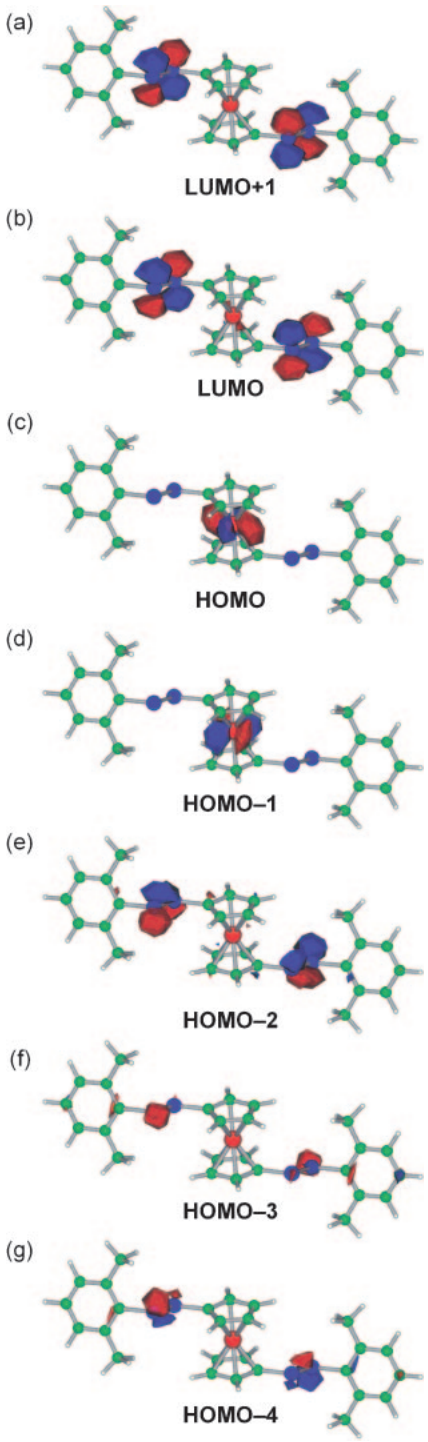

Fig. 10. Perspective views of the selected molecular orbitals of (*E*,*E*)-**8a** (white; hydrogen, green; carbon, blue; phosphorus, red; iron).

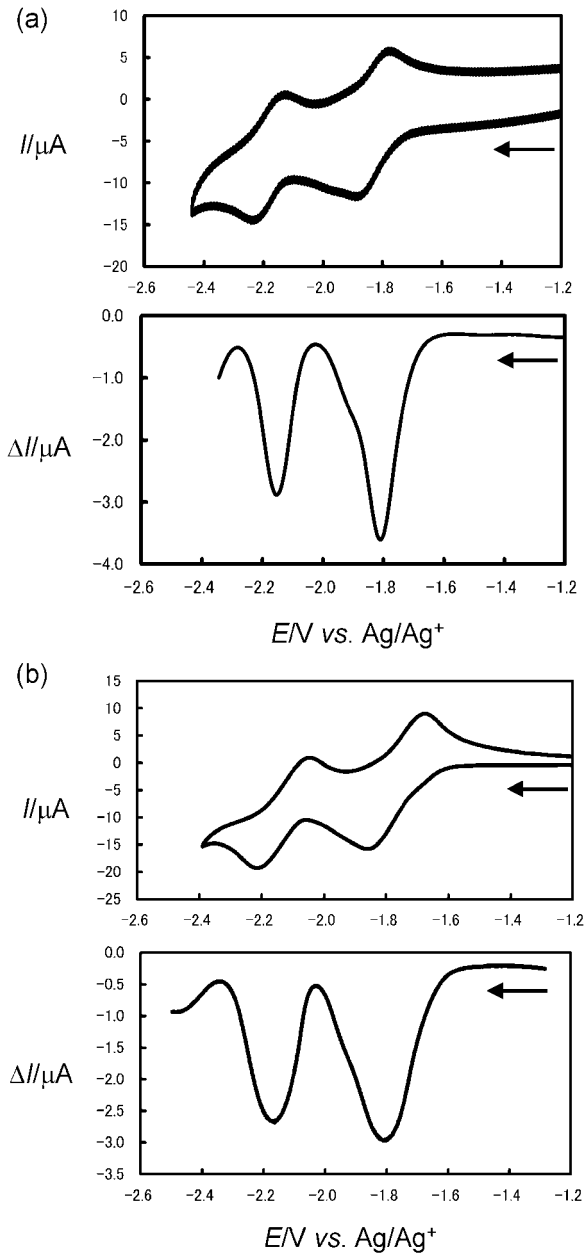

Fig. 11. Cyclic and differential pulse voltammograms of (a) (*E*,*E*)-**1a** and (b) (*E*,*E*)-**1b** in 0.1 M *n*-Bu_4NBF_4/THF solution at room temperature.

electron-transfer sites, afforded a comproportionation constant (K_c) of 8.2×10^5 for the mixed-valence state, indicating effective electronic interaction through the central ferrocene unit to similar extent of the case of the previously reported 1,4-bis[(*E*)-diphosphenyl]benzene (*E*,*E*)-**3a** ($\Delta E_{1/2} = 0.34$ V and $K_c = 5.6 \times 10^5$ in THF–*n*-Bu_4NBF_4).[7b] By contrast, it has been reported that no interaction is observed between the intramolecular diphosphene moieties of bis[(*E*)-diphosphene] **2** having an *o*-phenylene–ethylene–*o*-phenylene spacer (Fig. 2).[13] In CH_2Cl_2 solution, the reversible one-electron oxidation waves due to the iron(II)/iron(III) of the ferrocene moieties were observed at +0.14 V ((*E*,*E*)-**1a**) and +0.15 V ((*E*,*E*)-**1b**) versus Ag/Ag^+, respectively. These potentials are slightly lower than that of a ferrocene (+0.24 V versus Ag/Ag^+), indicating the influence of the polarized resonance structures, depicted in Fig. 5.

Reactions of the 1,1′-Bis[(*E*)-diphosphenyl]ferrocenes, (*E*,*E*)-1a and (*E*,*E*)-1b, with Methanol. In order to elucidate their reactivity, we reacted (*E*,*E*)-**1a** or (*E*,*E*)-**1b** with methanol. A benzene-d_6 solution of (*E*,*E*)-**1a**/(*E*,*E*)-**1b** was mixed with methanol in a sealed tube affording H_2PTbt (**4a**)/H_2-

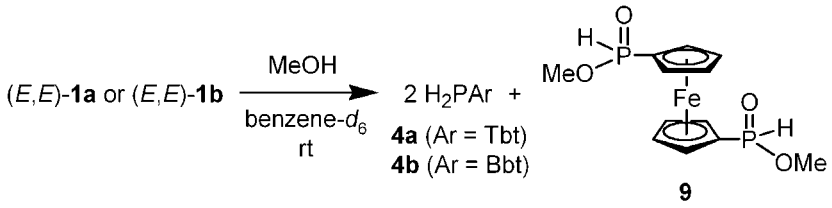

Scheme 2. Reactions of (*E*,*E*)-**1a** and (*E*,*E*)-**1b** with methanol in benzene-d_6.

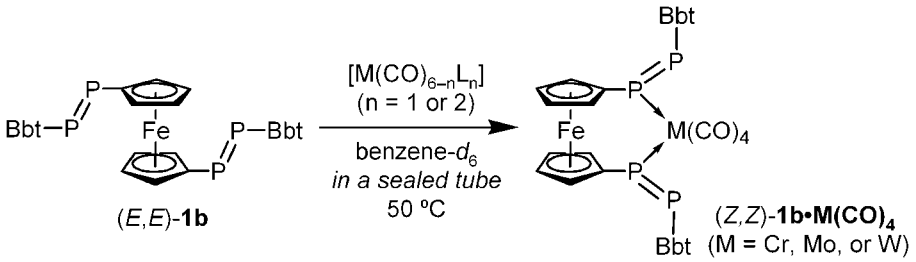

Scheme 3. Reactions of (*E*,*E*)-**1b** with group 6 metals carbonyl complexes.

Table 7. Redox Potentials (V vs. Ag/Ag^+) of (*E*,*E*)-**1a** and (*E*,*E*)-**1b**

		(*E*,*E*)-**1a**	(*E*,*E*)-**1b**
Oxidation[a]	E_{pa}	+0.17	+0.18
	E_{pc}	+0.10	+0.12
	$E_{1/2}$	+0.14	+0.15
Reduction[b]	E_{pc}	−2.02, −2.35	−1.89, −2.24
	E_{pa}	−1.66, −2.02	−1.67, −2.02
	$E_{1/2}$	−1.84, −2.19	−1.78, −2.13
	$\Delta E_{1/2}$	0.35	0.35
	Kc[c]	8.2×10^5	8.2×10^5

a) 0.1 M n-Bu_4NBF_4 in CH_2Cl_2, $E_{1/2}(Cp_2Fe/Cp_2Fe^+)$ = +0.24 V vs. Ag/Ag^+. b) 0.1 M n-Bu_4NBF_4 in THF. c) Comproportionation constant (K_c) was calculated by using the equation of $K_c = \exp(\Delta E_{1/2}/25.69)$ at 298 K.[17]

PBbt (**4b**) and $[Fe\{C_5H_4PH(O)OMe\}_2]$ (**9**) in a ratio of 2:1 (Scheme 2). The regioselectivity observed for the addition of methanol to the phosphorus–phosphorus double bonds of (*E*,*E*)-**1a**/(*E*,*E*)-**1b** can be interpreted in terms of the polarized resonance structure in solution as shown in Fig. 5.

Reactions of the 1,1′-Bis[(*E*)-diphosphenyl]ferrocene, (*E*,*E*)-1b, with Group 6 Metal Complexes. Next, we focused on the coordination behavior of (*E*,*E*)-**1b** to group 6 metal carbonyl complexes. Although a number of reports on diphosphene–group 6 metal carbonyl complexes have been published, the coordination properties of bis(diphosphene) derivatives have not been reported to the best of our knowledge. Because of a variety of coordination modes in metal complexes bearing a diphosphene unit (Fig. 4), 1,1′-bis[(*E*)-diphosphenyl]ferrocene ligand has attracted much interest not only in coordination chemistry but also in catalytic chemistry. On the other hand, experimental results have shown that the rotation energy of the cyclopentadienyl rings in ferrocene is about 4.6–9.6 kJ mol^{-1},[18] and therefore, free rotation readily occurs at room temperature in solution. Thus, the diphosphene units of the 1,1′-bis[(*E*)-diphosphenyl]ferrocene can move around an axis through the iron atom and the centroid of the cyclopentadienyl rings, indicating the possibility of forming a new architecture of metal complexes.

Table 8. Reactions of 1,1′-Bis[(*E*)-diphosphenyl]ferrocene (*E*,*E*)-**1b** with Group 6 Metal Carbonyl Complexes

Entry	Metal reagent	Product	Isolated yield/%
1	$[Cr(CO)_5(CH_3CN)]$	(*Z*,*Z*)-**1b·Cr(CO)$_4$**	81
2	$[Mo(CO)_4(nbd)]$[a]	(*Z*,*Z*)-**1b·Mo(CO)$_4$**	74
3	$[Mo(CO)_5(CH_3CN)]$	(*Z*,*Z*)-**1b·Mo(CO)$_4$**	70
4	$[W(CO)_4(cod)]$[b]	(*Z*,*Z*)-**1b·W(CO)$_4$**	89
5	$[W(CO)_5(CH_3CN)]$	(*Z*,*Z*)-**1b·W(CO)$_4$**	92

a) nbd; 2,5-norbornadiene. b) cod; 1,5-cyclooctadiene.

After heating a benzene-d_6 solution of 1,1′-bis[(*E*)-diphosphenyl]ferrocene (*E*,*E*)-**1b** in the presence of a 10 molar amount of $[Mo(CO)_4(nbd)]$ (nbd = 2,5-norbornadiene) at 50 °C for 2 h under the dark conditions, the signals for (*E*,*E*)-**1b** disappeared, and those for the molybdenum complex (*Z*,*Z*)-**1b·Mo(CO)$_4$** were exclusively observed in the ^1H and ^{31}P NMR spectra (Scheme 3 and Entry 2 in Table 8). Purification of the reaction mixture by gel-permeation chromatography afforded (*Z*,*Z*)-**1b·Mo(CO)$_4$** as a purple solid in 74% isolated yield. The ^1H NMR spectrum of (*Z*,*Z*)-**1b·Mo(CO)$_4$** in benzene-d_6 showed A_2B_2 signals and a broad singlet for the protons of the cyclopentadienyl and benzene rings of (*Z*,*Z*)-**1b·Mo(CO)$_4$** at 4.32, 4.62, and 6.92 ppm, respectively. The spectral features indicated the symmetric molecular structure of (*Z*,*Z*)-**1b·Mo(CO)$_4$** with C_2 axis passing through the iron and molybdenum atoms. In the ^{31}P NMR spectrum (Fig. 12), (*Z*,*Z*)-**1b·Mo(CO)$_4$** showed an AA′BB′ spin system at 358.7 and 304.3 ppm with $^1J(P_A–P_B) = \pm 606.7$, $^2J(P_A–P_{A'}) = \pm 29.7$, $^3J(P_A–P_{B'}) = \mp 14.9$, and $|^4J(P_B–P_{B'})| < 4.0$ Hz (Table 9), showing a higher field chemical shifts and a larger coupling constant $^1J_{PP}$ as compared to those for (*E*,*E*)-**1b** (491.1 and 496.9 ppm and $^1J_{PP} = 550$ Hz). On the basis of the spectroscopic properties of the previously reported complexes, $[M(CO)_5\{(Z)\text{-RP=PMes*}\}]$ (M = Cr, Mo, or W, R =

Table 9. ^{31}P NMR Data (Chemical Shifts in ppm and Coupling Constants in Hz) of (*Z*,*Z*)-**1b·Cr(CO)$_4$**, (*Z*,*Z*)-**1b·Mo(CO)$_4$**, and (*Z*,*Z*)-**1b·W(CO)$_4$** in Benzene-d_6

Complex	Spin system	δ_P	$^1J(P_A–P_B)$	$^2J(P_A–P_{A'})$	$^3J(P_A–P_{B'})$	$\lvert^4J(P_B–P_{B'})\rvert$
(*Z*,*Z*)-**1b·Cr(CO)$_4$**	AA′BB′	386.4, 295.9	±620.1	±37.3	∓18.7	<4.0
(*Z*,*Z*)-**1b·Mo(CO)$_4$**	AA′BB′	358.7, 304.3	±606.7	±29.7	∓14.9	<4.0
(*Z*,*Z*)-**1b·W(CO)$_4$**	AA′BB′	307.2[a], 283.7	±604.6	±29.0	∓14.5	<4.0

a) The resonance with the satellite signals of $^1J(^{183}W–^{31}P) = 245.1$ Hz.

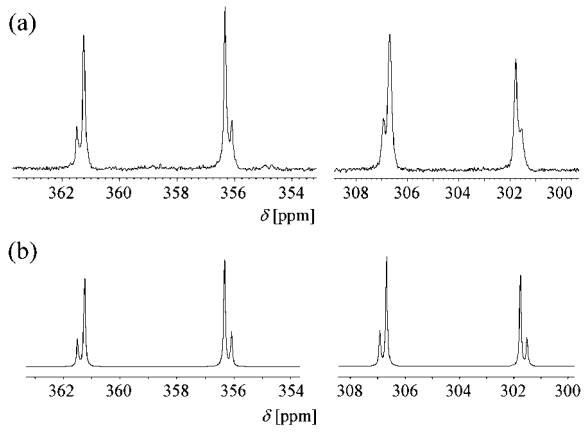

Fig. 12. (a) ^{31}P NMR spectrum of molybdenum complex (*Z*,*Z*)-**1b·Mo(CO)$_4$** in benzene-d_6. (b) The simulated resonance of an AA′BB′ spin system at 358.7 and 304.3 ppm with $^1J(P_A–P_B) = \pm606.7$, $^2J(P_A–P_{A'}) = \pm29.7$, $^3J(P_A–P_{B'}) = \mp14.9$, $|^4J(P_B–P_{B'})| < 4.0$ Hz (line width of 8.0 Hz).

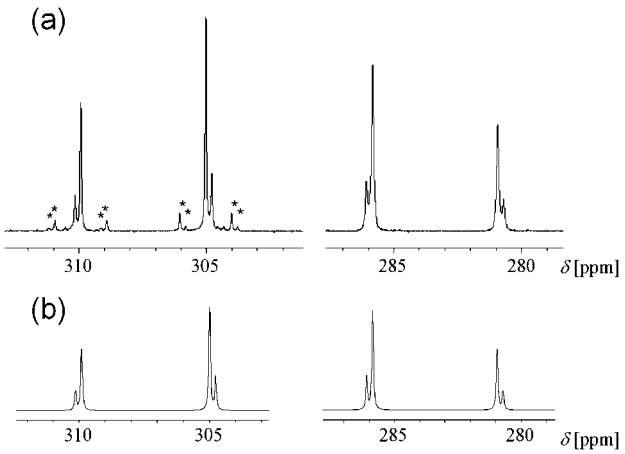

Fig. 13. (a) ^{31}P NMR spectrum of tungsten complex (*Z*,*Z*)-**1b·W(CO)$_4$** in benzene-d_6. The asterisk indicates the tungsten–phosphorus satellite signals of $^1J(^{183}W–^{31}P)$ (245.1 Hz). (b) The simulated resonance of an AA′BB′ spin system at 307.2 and 283.7 ppm with $^1J(P_A–P_B) = \pm604.6$, $^2J(P_A–P_{A'}) = \pm29.0$, $^3J(P_A–P_{B'}) = \mp14.5$, $|^4J(P_B–P_{B'})| < 4.0$ Hz (line width of 8.0 Hz).

Table 10. ^{31}P NMR Data of [M(CO)$_5${(*Z*)-RP=PRMes*}]

R	M	δ_P/ppm	$^1J_{PP}$
Mes	Cr	384.9, 393.9	603.0
Mes	Mo	359.0, 398.4	585.9
Mes	W	322.4[a], 393.1	576.8
Cp*	Cr	421, 385	603
Cp*	Mo	396, 391	583
Cp*	W	394, 362	581

a) The resonance with the satellite signals of $^1J(^{183}W–^{31}P) = 231.9$ Hz.

Mes or Cp*) (Table 10),[19] these spectral features suggest that (*Z*,*Z*)-**1b·Mo(CO)$_4$** possesses (*Z*)-configurated P=P units in spite of the (*E*)-configuration of the staring material (*E*,*E*)-**1b**. Furthermore, the observed $^2J(P_A–P_{A'})$ (±29.7 Hz) and $^3J(P_A–P_{B'})$ (∓14.9 Hz) values suggested that only two phosphorus atoms of (*Z*,*Z*)-**1b·Mo(CO)$_4$** coordinate to the molybdenum metal with a cis conformation, based on the former coupling constant $^2J(P_A–P_{A'})$. The values are close to those of the reported compounds *cis*-[Mo(CO)$_4$(PR$_3$)(PR′$_3$)] (23–33 Hz).[20]

Similarly, in the case of (*Z*,*Z*)-**1b·Mo(CO)$_4$**, the novel tungsten complex (*Z*,*Z*)-**1b·W(CO)$_4$**, [W(CO)$_4${(*Z*,*Z*)-(BbtP=PC$_5$H$_4$)$_2$Fe}], was obtained as purple crystals in 89% isolated yield, when a 10 molar amount of [W(CO)$_4$(cod)] (cod = 1,5-cyclooctadiene) was used as the metal source in benzene-d_6 (Scheme 3 and Entry 4 in Table 8). A ^{31}P NMR spectrum of (*Z*,*Z*)-**1b·W(CO)$_4$** in benzene-d_6 showed characteristic signals of an AA′BB′ spin system at 307.2 and 283.7 ppm with $^1J(P_A–P_B) = \pm604.6$, $^2J(P_A–P_{A'}) = \pm29.0$, $^3J(P_A–P_{B'}) = \mp14.5$, and $|^4J(P_B–P_{B'})| < 4.0$ Hz (Fig. 13 and Table 9). It should be noted that the former resonance ($\delta_P = 307.2$) of (*Z*,*Z*)-**1b·W(CO)$_4$** has satellite signals with $^1J(^{183}W–^{31}P) = 245.1$ Hz, which lies within the range of the reported values for the tungsten complexes coordinated to a low-coordinated phosphorus atom,[10d,11a,11d–f,13,19b,19c,21–23] suggesting that the two diphosphene units should coordinate to the tungsten metal in an η^1-fashion (end-on) in solution.

Finally, a systematic method for the synthesis of group 6 metal complexes of (*E*,*E*)-**1b** was established by using of [M(CO)$_5$(CH$_3$CN)] (M = Cr, Mo, and W), which can be readily prepared from the commercially available reagents, [M(CO)$_6$].[24,25] That is, the treatment of (*E*,*E*)-**1b** with an excess amount (at least 10 molar amount) of [M(CO)$_5$(CH$_3$CN)] (M = Cr, Mo, and W) afforded (*Z*,*Z*)-**1b·Cr(CO)$_4$**, (*Z*,*Z*)-**1b·Mo(CO)$_4$**, and (*Z*,*Z*)-**1b·W(CO)$_4$** in 81%, 70%, and 92% isolated yields, respectively (Scheme 3 and Entries 1, 3, and 5 in Table 8). A ^{31}P NMR spectrum of (*Z*,*Z*)-**1b·Cr(CO)$_4$** is shown in Fig. 14 together with its simulated one. All ^{31}P NMR data of (*Z*,*Z*)-**1b·Cr(CO)$_4$**, (*Z*,*Z*)-**1b·Mo(CO)$_4$**, and (*Z*,*Z*)-**1b·W(CO)$_4$** are summarized in Table 9. The features of these complexes in the ^{31}P NMR spectra agreed with those

of the previously reported η^1-complexes of (*Z*)-diphosphene with a group 6 metal, as shown in Table 10.[5,19,26] Moreover, the observed $^1J_{PP}$ values (620.1 Hz for (*Z*,*Z*)-**1b·Cr(CO)$_4$**, 606.7 Hz for (*Z*,*Z*)-**1b·Mo(CO)$_4$**, and 604.6 Hz for (*Z*,*Z*)-**1b·W(CO)$_4$**) were larger than that of (*E*,*E*)-**1b** (550 Hz), indicating the enhanced s-character of the double bond in the diphosphene moieties.

Although (*E*)-diphosphene η^1-metal complexes have been reported to undergo photochemical isomerization leading to the formation of the corresponding (*Z*)-diphosphene η^1-metal complexes,[1a,5,19] the thermal isomerization has been hitherto unknown. Therefore, we tried to explore the isomerization process depending on the amount of the metal reagents in the ligand-exchange reactions. Treatment of (*E*,*E*)-**1b** with a 5 molar amount of [W(CO)$_5$(CH$_3$CN)] in benzene-d_6 at 50 °C for 2 h resulted in the formation of the mixture of two isomers in the ratio (*E*,*Z*)-**1b·W(CO)$_4$**:(*Z*,*Z*)-**1b·W(CO)$_4$** = 1:3 as judged by the ^{1}H and ^{31}P NMR spectra (Fig. 15). Consequently, these results suggest that the unique *E*-to-*Z* isomerization process of the diphosphene moieties in (*E*,*E*)-**1b** depends on the ratio of the metal reagents. Moreover, in order to investigate the effect of the ferrocenyl group, the ligand-exchange reaction of (*E*)-FcP=PTbt, with [Cr(CO)$_5$(thf)] was also examined in the dark.[27] It is interesting that the reaction of (*E*)-FcP=PTbt with an excess molar amount of [Cr(CO)$_5$(thf)] at room temperature afforded only [Cr(CO)$_5${(*Z*)-FcP=PTbt}] in 73% yield along with *E*-to-*Z* isomerization. The results indicate: (i) the Tbt group prevents the adjacent phosphorus atom from coordination to the chromium atom due to its extreme hindrance, and (ii) the isomerization of the diphosphene moiety having a ferrocenyl group proceeds at room temperature during the ligand-exchange reaction in the presence of an excess amount of [Cr(CO)$_5$(thf)].

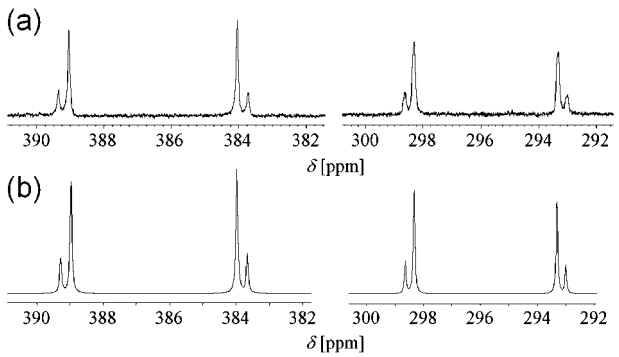

Fig. 14. (a) ^{31}P NMR spectrum of chromium complex (*Z*,*Z*)-**1b·Cr(CO)$_4$** in benzene-d_6. (b) The simulated resonance of an AA′BB′ spin system at 386.4 and 295.9 ppm with $^1J(P_A–P_B) = \pm620.1$, $^2J(P_A–P_{A'}) = \pm37.3$, $^3J(P_A–P_{B'}) = \mp18.7$, $|^4J(P_B–P_{B'})| < 4.0$ Hz (line width of 8.0 Hz).

The observed *E*-to-*Z* isomerization process of the diphosphene units of (*E*,*E*)-**1b** in the dark is probably due to the use of an excess molar amount of the metal reagents and the contribution of the polarized resonance structure of (*E*,*E*)-**1b** (Fig. 5), which should make the rotation barrier of the P=P double bond lower than those of diaryldiphosphenes having no π-conjugation system between the diphosphene and the aryl groups.

Infrared Spectra of the 1,1′-Bis[(*Z*)-diphosphenyl]ferrocene–Group 6 Metal Complexes. There have been numerous reports for the IR spectra of group 6 metal carbonyl complexes, and the studies using IR spectroscopy give useful information to understand the electronic structure of the complexes. On the other hand, a combination of IR spectroscopy and theoretical calculations can be a powerful tool for investigating the molecular structure and bonding properties of the complexes.[28] In general, local C_{2v} symmetry in *cis*-[M(CO)$_4$L$_2$] (M = group 6 metals, L = ligands) leading to four carbonyl stretching modes (2A$_1$, B$_1$, and B$_2$).[29] The IR spectra of (*Z*,*Z*)-**1b·Cr(CO)$_4$**, (*Z*,*Z*)-**1b·Mo(CO)$_4$**, and (*Z*,*Z*)-**1b·W(CO)$_4$** were recorded as Nujol samples and the results are summarized in Table 11 together with those of the previously reported tetracarbonyl complexes *cis*-[M(CO)$_4$L$_2$]. The IR spectra of (*Z*,*Z*)-**1b·Cr(CO)$_4$**, (*Z*,*Z*)-**1b·Mo(CO)$_4$**, and (*Z*,*Z*)-**1b·W(CO)$_4$** showed four strong absorptions attributable to the C≡O stretching frequency in the range of 2030–1900 cm^{-1}, indicating a cis geometry around the metal moieties in (*Z*,*Z*)-**1b·Cr(CO)$_4$**, (*Z*,*Z*)-**1b·Mo(CO)$_4$**, and (*Z*,*Z*)-**1b·W(CO)$_4$**. These bands were similar to those of 2,2′-biphosphorin molybdenum **10**[10e] and di(phosphaalkene) complexes **11**–**13**[11e] and found to be shifted toward higher frequencies by 6–34 cm^{-1} as compared to those of *cis*-[M(CO)$_4${(PPh$_2$CH$_2$)$_2$}] (M = Cr, Mo, and W)[30] (Fig. 16). These results indicate the σ-donor and π-acceptor abilities of the (*Z*,*Z*)-**1b** ligand may resemble those of 2,2′-biphosphorin and di(phosphaalkene) ligands having low-coordinated phosphorus atoms.

Crystal Structure of (*Z*,*Z*)-1b·W(CO)$_4$. Since only one example [Cr(CO)$_5${(*Z*)-MesP=PMes*}] has been reported for the solid-state structure of the diphosphene mono-metal η^1-complex bearing group 6 metal so far,[19a] the structural features of the group 6 metal complex of the 1,1′-bis[(*Z*)-diphosphenyl]ferrocene are of great interest. The molecular

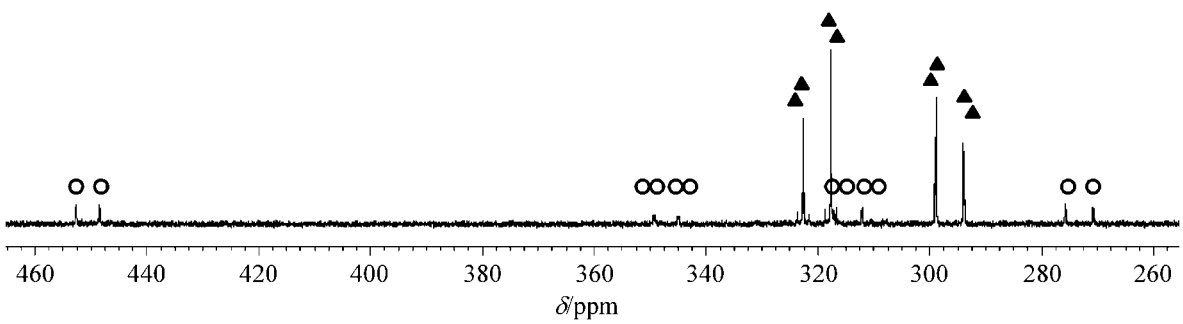

Fig. 15. ^{31}P NMR spectrum of (*E*,*Z*)-**1b·W(CO)$_4$** (open circle) and (*Z*,*Z*)-**1b·W(CO)$_4$** (solid triangle) in benzene-d_6.

Table 11. IR Data of *cis*-Group 6 Metal Tetracarbonyl Complexes

Complex	ν/cm^{-1}	Ref.
(*Z*,*Z*)-**1b·Cr(CO)$_4$**[a]	2015, 1954, 1935, 1910	this work
(*Z*,*Z*)-**1b·Mo(CO)$_4$**[a]	2028, 1958, 1942, 1906	this work
(*Z*,*Z*)-**1b·W(CO)$_4$**[a]	2024, 1951, 1932, 1896	this work
10[a]	2030, 1935, 1900	11e
11[b]	2013, 1957, 1923, 1892	12e
12[b]	2025, 1928, 1892	12e
13[b]	2019, 1919, 1888	12e
cis-[Cr(CO)$_4${(PPh$_2$CH$_2$)$_2$}][c]	2009, 1914, 1899, 1877	28
cis-[Mo(CO)$_4${(PPh$_2$CH$_2$)$_2$}][c]	2020, 1919, 1907, 1881	28
cis-[W(CO)$_4${(PPh$_2$CH$_2$)$_2$}][c]	2016, 1912, 1901, 1876	28

a) Nujol method. b) KBr method. c) 1,2-Dichloroethane solution.

Table 12. Selected Structural Parameters of (*Z*,*Z*)-**1b·W(CO)$_4$**

Bond lengths/Å		Bond angles/deg		Torsion angles/deg	
P(1)–P(2)	2.038(6)	C(1)–P(1)–P(2)	118.2(5)	C(1)–P(1)–P(2)–C(15)	9.7(7)
P(3)–P(4)	2.046(5)	C(15)–P(2)–P(1)	113.9(5)	C(6)–P(3)–P(4)–C(45)	4.1(8)
P(1)–C(1)	1.775(14)	C(6)–P(3)–P(4)	116.7(5)		
P(3)–C(6)	1.776(16)	C(45)–P(4)–P(3)	119.3(4)		
P(2)–C(15)	1.800(16)	C(1)–P(1)–W(1)	124.2(5)		
P(4)–C(45)	1.830(13)	P(2)–P(1)–W(1)	117.6(2)		
W(1)–P(1)	2.414(4)	C(6)–P(3)–W(1)	125.3(5)		
W(1)–P(3)	2.422(4)	P(4)–P(3)–W(1)	118.0(2)		

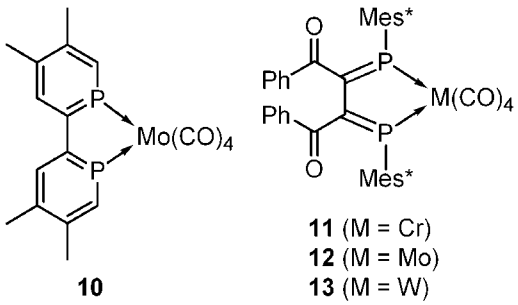

Fig. 16.

structure of (*Z*,*Z*)-**1b·W(CO)$_4$** was determined by X-ray crystallographic analysis. An ORTEP drawing of the major part of the disordered molecules and the selected structural parameters of (*Z*,*Z*)-**1b·W(CO)$_4$** are described in Fig. 17 and Table 12, respectively. Based on spectroscopic analyses with the almost planar C–P–P–C torsion angles (4.1(8) and 9.7(7)°), it was found that the two diphosphene moieties of (*Z*,*Z*)-**1b·W(CO)$_4$** has a *Z*-configuration as expected and the two phosphorus atoms adjacent to the central ferrocene moiety coordinated to the tetracarbonyl tungsten are in a cis form. The phosphorus–phosphorus bond lengths of (*Z*,*Z*)-**1b·W(CO)$_4$** (2.038(6) and 2.046(5) Å) are substantially shorter than the typical P–P single-bond length (ca. 2.19–2.24 Å),[14] whereas they are within the range of the reported P=P double-bond lengths (1.985–2.049 Å) for (*E*)-diphosphenes,[1a,4f,4h,4l] and very close to that (2.039(3) Å) of the (*Z*)-diphosphene–chromium complex [Cr(CO)$_5${(*Z*)-MesP=PMes*}].[19a] These results show that (*Z*,*Z*)-**1b·W(CO)$_4$** retains considerable P=P double-bond character with a *Z*-configuration in the solid state. The phosphorus–phosphorus bond lengths of (*Z*,*Z*)-

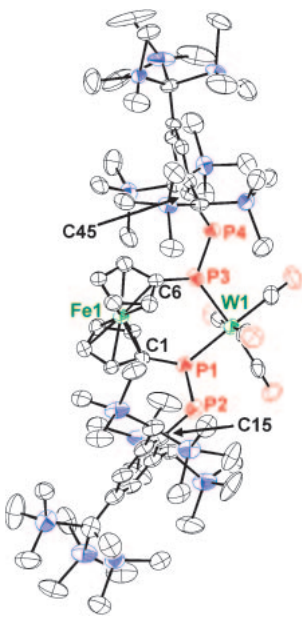

Fig. 17. ORTEP drawing of the major part of (*Z*,*Z*)-**1b·W(CO)$_4$** with thermal ellipsoid plots (30% probability). Hydrogen atoms are omitted for clarity.

1b·W(CO)$_4$ were slightly longer than that of (*E*,*E*)-**1b**, suggesting relatively weak d_W–$\pi^*_{P=P}$ back donation from d orbitals of the tungsten atom to π^* orbitals of the P=P bonds. Moreover, the six P–W–C and four C–W–C angles are in the range from 88.3(5) to 93.5(4)° and from 87.9(7) to 93.3(6)°, respectively, where the tungsten center of (*Z*,*Z*)-**1b·W(CO)$_4$** adopts an octahedral geometry with a P–W–P angle of 90.60(12)°. This indicates low steric strain around the tungsten

center, in contrast to those found for the reported tungsten complexes bearing a bidentate phosphorus ligand.[22,23] The P(1) and P(3) atoms coordinated toward the tungsten atom were found to have completely planar geometries (the sum of the angles around the P(1) and P(3) atoms are 360.0°) as in the case of [Cr(CO)$_5${(*Z*)-MesP=PMes*}] (359.9°). The P(2)–P(1)–C(1) and P(4)–P(3)–C(6) bond angles (116.7(5) and 118.2(5)°) of (*Z*,*Z*)-**1b·W(CO)$_4$** are larger than those of (*E*,*E*)-**1b** (102.6(3)°) and similar to that of [Cr(CO)$_5${(*Z*)-MesP=PMes*}] (118.7(3)°), indicating a large amount of sp^2-hybridized character in the P–P bonds (P(1)–P(2) and P(3)–P(4)) in (*Z*,*Z*)-**1b·W(CO)$_4$** as compared to that in (*E*,*E*)-**1b**. To our best knowledge, the phosphorus–tungsten(0) bond lengths of (*Z*,*Z*)-**1b·W(CO)$_4$** [2.414(4) and 2.422(4) Å] are considerably shorter than those of the reported tungsten complexes coordinated by sp^3- and sp^2-type phosphorus atoms,[11d–f,13,20c,22,23] except for the tungsten complex of tris(tetramethyl-2,2′-biphosphorin) (2.3552(9), 2.361(1), and 2.3640(6) Å).[10d] These results of the structural properties in (*Z*,*Z*)-**1b·W(CO)$_4$** indicate the following: (i) a good σ-donating ability of the lone-pair electrons in the diphosphene units with complexation in a η^1-fashion (end-on), (ii) a flexible 1,1′-ferrocenylene moiety and selective formation of the bidentate complexes due to the two extremely bulky Bbt groups, (iii) complexation of the diphosphene moieties with an sp^2-hydridized geometry, and (iv) a slightly longer P=P bond lengths indicating their relatively weak d–π^* back donation from the central tungsten atom.

UV–Vis Spectra of (*Z*,*Z*)-1b·Cr(CO)$_4$, (*Z*,*Z*)-1b·Mo(CO)$_4$, and (*Z*,*Z*)-1b·W(CO)$_4$. UV–vis spectra of (*Z*,*Z*)-**1b·Cr(CO)$_4$**, (*Z*,*Z*)-**1b·Mo(CO)$_4$**, and (*Z*,*Z*)-**1b·W(CO)$_4$** were measured in hexane (Fig. 18), showing approximately two characteristic absorption maxima in the range from 300 to 800 nm. Since there has been no report for the electronic spectral data of group 6 metal complexes of (*Z*)-diphosphenes and it is difficult to make an assignment for their electronic transitions, the assignment were estimated based on TDDFT calculations on a model molecule, [Cr(CO)$_4${(*Z*,*Z*)-(HP=PC$_5$H$_4$)$_2$Fe}] ((*Z*,*Z*)-**14**) (vide infra). The absorption maxima observed at shorter wavelength (λ_{max} = 360 (sh, ε = 4400) for (*Z*,*Z*)-**1b·Cr(CO)$_4$**, 362 (sh, ε = 5400) for (*Z*,*Z*)-**1b·Mo(CO)$_4$**, and 363 nm (sh, ε = 4400) for (*Z*,*Z*)-**1b·W(CO)$_4$**) can be assigned to the $\pi \rightarrow \pi^*$ electron transitions for the diphosphene units taking into account those for the previously reported (*E*)-diaryldiphosphenes ($\pi \rightarrow \pi^*$ band; 277–418 nm)[1a] and [Cr(CO)$_5${(*Z*)-FcP=PTbt}] (λ_{max} = 352 nm).[27] The absorption maxima observed at longer wavelength (λ_{max} = 492 (ε = 5400), 640 (sh, ε = 1300) for (*Z*,*Z*)-**1b·Cr(CO)$_4$**, 488 (ε = 4100), 627 (sh, ε = 640) for (*Z*,*Z*)-**1b·Mo(CO)$_4$**, and 492 (ε = 5700), 620 (sh, ε = 1500) nm for (*Z*,*Z*)-**1b·W(CO)$_4$**), which were very broad, can be attributed to the mixture of several types of d $\rightarrow \pi^*$ (MLCT) bands due to the electron transitions from the d orbitals of the iron and group 6 metal atoms to the π^* orbitals of the P=P moieties, respectively. Moreover, the MLCT bands exhibited a bathochromic shift as compared to that for the 1,1′-bis[(*E*)-diphosphenyl]ferrocene (*E*,*E*)-**1b** (λ_{max} = 553 nm).

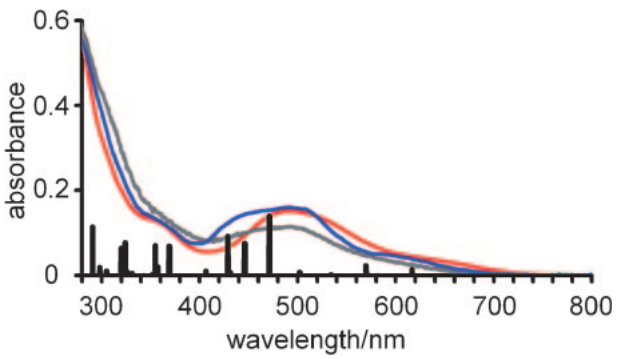

Fig. 18. UV–vis spectra of (*Z*,*Z*)-**1b·Cr(CO)$_4$** (red line), (*Z*,*Z*)-**1b·Mo(CO)$_4$** (gray line), and (*Z*,*Z*)-**1b·W(CO)$_4$** (blue line) in hexane and the calculated electron transitions (black bars) for the excited state of [Cr(CO)$_4${(*Z*,*Z*)-(HP=PC$_5$H$_4$)$_2$Fe}] ((*Z*,*Z*)-**14**).

Theoretical Calculations for 1,1′-Bis[(*Z*)-diphosphenyl]-ferrocene–Chromium Tetracarbonyl Complex. Structural optimization on [Cr(CO)$_4${(*Z*,*Z*)-(HP=PC$_5$H$_4$)$_2$Fe}] ((*Z*,*Z*)-**14**), as a model molecule, was performed at B3LYP/6-31G(d) level using an initial geometry referred to the solid-state structure of (*Z*,*Z*)-**1b·W(CO)$_4$**. The theoretically optimized coordinates and selected molecular orbitals of (*Z*,*Z*)-**14** are summarized in the Supporting Information (Tables S4 and S6). The optimized structure of (*Z*,*Z*)-**14** was found to have a geometry similar to the solid-state structure of (*Z*,*Z*)-**1b·W(CO)$_4$**. The low-lying LUMO and LUMO+1 for (*Z*,*Z*)-**14** had $\pi^*_{P=P}$ character as in the case of [Fe(C$_5$H$_4$P=PDmp)$_2$] (*E*,*E*)-**8a** (Table S6). Furthermore, the HOMO, HOMO−1, and HOMO−2 of (*Z*,*Z*)-**14** were localized on the d orbitals of the chromium atom, whereas all of the orbitals from the HOMO−3 to the HOMO−6 should be d orbitals of the iron atom of the ferrocene unit. In addition, TDDFT calculations on (*Z*,*Z*)-**14** were also performed at TD-B3LYP/6-31G(d) level. The calculated low-lying singlet excitation energies of (*Z*,*Z*)-**14** are shown in the Supporting Information (Table S5). The lowest energy part (between 617.3 and 357.3 nm) of the calculations on (*Z*,*Z*)-**14** originated from electron transitions from the d orbitals of the iron and group 6 metals into the low-lying $\pi^*_{P=P}$ orbitals (MLCT transitions), whereas the excitations in the range of 354.6 to 291.4 nm were due to allowed transitions from the $\pi_{P=P}$ to the $\pi^*_{P=P}$ and forbidden transitions from the $n_{P=P}$ to the $\pi^*_{P=P}$ orbitals. The computational results indicate that the predicted energies of the singlet excitations of (*Z*,*Z*)-**14** are in good agreement with the experimental results.

Conclusion

We synthesized the first stable 1,1′-bis[(*E*)-diphosphenyl]-ferrocenes (*E*,*E*)-**1a** and (*E*,*E*)-**1b** by taking advantage of bulky protecting groups, Tbt and Bbt. Compounds (*E*,*E*)-**1a** and (*E*,*E*)-**1b** are very robust in an inert atmosphere. The ^{31}P NMR spectra of (*E*,*E*)-**1a** and (*E*,*E*)-**1b** showed diagnostic AB systems in a characteristic low-field region, suggesting the formation of phosphorus–phosphorus double bonds with the asymmetric substituents. Solid-state Raman and IR spectra of (*E*,*E*)-**1a** and (*E*,*E*)-**1b** also indicated characteristic stretching vibrations of the P=P units as well as their NMR spectra in solution. The molecular structures of (*E*,*E*)-**1a** and (*E*,*E*)-**1b** were

established by X-ray crystallographic analyses, and the double-bond character of (*E*,*E*)-**1a** and (*E*,*E*)-**1b** was elucidated. The UV–vis spectra of (*E*,*E*)-**1a** and (*E*,*E*)-**1b** showed three types of absorptions, which corresponded to the $\pi \rightarrow \pi^*$, n $\rightarrow$ π^*, and d $\rightarrow \pi^*$ electron transitions of (*E*,*E*)-**1a** and (*E*,*E*)-**1b**. The electrochemical properties of (*E*,*E*)-**1a** and (*E*,*E*)-**1b** were revealed by cyclic and differential pulse voltammetries. It is interesting that the two reversible one-electron redox waves due to the stepwise reductions of the P=P units of (*E*,*E*)-**1a** and (*E*,*E*)-**1b** were found in the range from about -1.8 to -2.2 V versus Ag/Ag^+. These results pointed out the electronic interaction between the diphosphene moieties through the central ferrocene units of (*E*,*E*)-**1a** and (*E*,*E*)-**1b**.

Furthermore, we observed unique ligand-exchange reactions of 1,1′-bis[(*E*)-diphosphenyl]ferrocene (*E*,*E*)-**1b** as a bidentate ligand having sp^2-type phosphorus atoms with group 6 metals leading to the formation of novel 1,1′-bis[(*Z*)-diphosphenyl]-ferrocene–metal complexes [$M(CO)_4${(*Z*,*Z*)-(BbtP=PC_5H_4)$_2$-Fe}] (M = Cr, Mo, or W). The molecular structure of the tungsten complex was determined by X-ray crystallographic analysis, showing that the diphosphene units have *Z*-configurations and coordinated to the tungsten metal with η^1-fashion. It should be noted that the diphosphene units of (*E*,*E*)-**1b** underwent an *E*-to-*Z* isomerization during complexation. It was also found that the progress of the ligand-exchange reactions depended on the ratio of the metal reagents. These results will stimulate further interest to understand the interactions between diphosphene units and group 6 metals. Several types of d $\rightarrow \pi^*_{P=P}$ electron transitions due to the iron and group 6 metals were detected by UV–vis spectroscopy, and these results were supported by theoretical calculations.

Experimental

General Comments. All experiments were performed under an argon atmosphere unless otherwise noted. All solvents were purified by standard methods and then dried by using an Ultimate Solvent System (Glass Contour Company).[31] All solvents used in the spectroscopy (benzene, benzene-d_6, and hexane) were dried by using a potassium mirror. Preparative thin-layer chromatography (PTLC) was performed with Merck Kieselgel 60 PF254. Preparative gel-permeation liquid chromatography (GPLC) was performed on an LC-908 or LC-918 apparatus equipped with JAI-gel 1H and 2H columns (Japan Analytical Industry Co., Ltd.) with toluene as an eluent. ^{1}H NMR (400 or 300 MHz) and ^{13}C NMR (100 or 75 Hz) spectra were measured in C_6D_6 with a JEOL AL-400 or -300 spectrometer using C_6HD_5 (δ 7.15) and C_6D_6 (δ 128.0) as internal standards for ^{1}H and ^{13}C NMR spectra, respectively. ^{31}P NMR (120 MHz) spectra were measured in C_6D_6 with a JEOL AL-300 spectrometer using 85% H_3PO_4 in water (δ 0) as an external standard. High-resolution EI- and FAB-mass spectral data were obtained on a JEOL SX-270 mass spectrometer (matrix: 2-nitrophenyl octyl ether). Electronic spectra were recorded on a JASCO V-570 UV/Vis spectrometer. Infrared spectra were obtained on a JASCO FT/IR-460 plus spectrometer. Raman spectra were measured on a Raman spectrometer consisting of an Spex 1877 Triplemate and an EG&G PARC 1421 intensified photodiode array detector. An NEC GLG 108 He-Ne laser was used for Raman excitation. The electrochemical experiments were carried out with an ALS 602A electrochemical analyzer using a glassy carbon disk working electrode, a Pt wire counter electrode, and Ag/0.01 M (1 M = 1 mol dm^{-3}) $AgNO_3$ reference electrode. The measurements were carried out in CH_2Cl_2 and THF solution containing 0.1 M *n*-Bu_4NBF_4 as a supporting electrolyte with scan rates of 10–200 mV s^{-1} in a glovebox filled with argon at ambient temperature. All melting points were determined on a Yanaco micro melting point apparatus and were uncorrected. Elemental analyses were performed by the Microanalytical Laboratory of the Institute for Chemical Research, Kyoto University.

Materials. Hydrogen chloride in ether was purchased from Aldrich Co., Ltd. Celite® (diatomacenous earth) was purchased from KANTO CHEMICAL Co., Inc. and dried at 200 °C for 24 h before use. 1,8-Diazabicyclo[5.4.0]undec-7-ene (DBU) was purchased from Aldrich Co., Ltd. and was distillated form sodium hydroxide prior to use. 2,4,6-Tris[bis(trimethylsilyl)methyl]phenylphosphine, H_2PTbt (**4a**),[4h] 1,1′-dibromoferrocene,[32] bis(diethylamino)chlorophosphine,[33] 1,1′-bis(dichlorophosphino)ferrocene,[34] and [$M(CO)_5(CH_3CN)$] (M = Cr, Mo, and W)[24,25] were prepared according to the procedures reported in the literatures. [$Mo(CO)_4$-(nbd)] (nbd = 2,5-norbornadiene) and [$W(CO)_4$(cod)] (cod = 1,5-cyclooctadiene) were purchased from Aldrich Co., Ltd. and purified by recrystallization from toluene before use.

Preparation of 2,6-Bis[bis(trimethylsilyl)methyl]-4-[tris(trimethylsilyl)methyl]phenylphosphine (4b). To a solution of 2,6-[bis(trimethylsilyl)methyl]-4-[tris(trimethylsilyl)methyl]phenyldichlorophosphine (2.00 g, 2.75 mmol) in THF (50 mL) was added lithium aluminum hydride (104 mg, 2.75 mmol) at 0 °C. The solution was stirred at 0 °C for 1 h and warmed to room temperature. After the solvent was removed, hexane was added to the residue. The suspension was filtered through Celite®, the resulting solution was filtered through a pad of silica gel to afford 2,6-bis[bis(trimethylsilyl)methyl]-4-[tris(trimethylsilyl)methyl]phenylphosphine (1.73 g, 2.63 mmol, 96%) as colorless solids. **4b**: mp 152.5–153.5 °C. ^{1}H NMR (300 MHz, $CDCl_3$, 23 °C) δ 0.05 (s, 27H, $Si(CH_3)_3$), 0.24 (s, 36H, $Si(CH_3)_3$), 2.49 (s, 1H, CH), 2.51 (s, 1H, CH), 3.68 (brd, 2H, $^1J_{PH}$ = 190 Hz, PH_2), 6.76 (s, 1H, C_6H_2), 6.77 (s, 1H, C_6H_2). ^{13}C{^{1}H} NMR (75 MHz, $CDCl_3$, 24 °C) δ 1.08 (s, CH_3), 5.31 (s, CH_3 × 2), 21.78 (s, *C*($SiMe_3$)$_3$), 30.65 (s, *C*H($SiMe_3$)$_2$), 30.78 (s, *C*H($SiMe_3$)$_2$), 122.62 (d, $^2J_{PC}$ = 3.1 Hz, *o*-C_6H_2), 126.30 (d, $^3J_{PC}$ = 1.9 Hz, *m*-C_6H_2), 143.98 (s, *p*-C_6H_2), 148.47 (d, $^1J_{PC}$ = 11.7 Hz, *ipso*-C_6H_2). ^{31}P NMR (120 MHz, $CDCl_3$, 24 °C) δ -142.4 (t, $^1J_{HP}$ = 190 Hz, PH_2). HRMS (FAB): *m*/*z* found 656.3543 ([M + H]$^+$), calcd for $C_{30}H_{69}PSi_7$: 656.3522. Anal. Calcd for $C_{30}H_{69}PSi_7$: C, 54.81; H, 10.58%. Found: C, 54.58; H, 10.37%.

Preparation of 1,1′-Bis[bis(diethylamino)phosphino]ferrocene (5). To a solution of 1,1′-dibromoferrocene (902 mg, 2.62 mmol) in ether (20 mL) was added butyllithium in hexane (1.50 mol dm^{-3}, 3.84 mL, 5.76 mmol) at -78 °C. The solution was warmed to room temperature for 30 min and was cooled to -78 °C. After bis(diethylamino)chlorophosphine (1.21 mL, 5.76 mmol) was added to the solution at -78 °C, the reaction mixture was allowed to be warmed to room temperature for 30 min and was stirred for 14 h. After removal of the solvents, hexane was added to the residue and the mixture was filtered through Celite®. The solvent of the filtrate was removed to afford 1,1′-bis[bis(diethylamino)phosphino]ferrocene (**5**) (1.37 g, 2.56 mmol, 98%) as an orange oil. **5**: ^{1}H NMR (300 MHz, C_6D_6, 25 °C) δ 1.03 (t, $^1J_{HH}$ = 6.8 Hz, CH_3, 24H), 3.00–3.10 (m, CH_2, 16H), 4.36 (A_2B_2, $^1J_{HH}$ = 1.8 Hz, C_5H_4, 4H), 4.37 (A_2B_2, $^1J_{HH}$ = 1.8 Hz, C_5H_4, 4H). ^{13}C{^{1}H} NMR (75 MHz, C_6D_6, 25 °C) δ 15.00 (d, $^2J_{CP}$ = 3.07 Hz, CH_3), 42.88 (d, $^1J_{CP}$ = 17.3 Hz, CH_2), 72.29 (s, CH), 72.73 (s, CH), 81.92 (d, $^1J_{CP}$ = 11.7 Hz, *ipso*-C_5H_4). ^{31}P NMR

(120 MHz, C_6D_6, 25 °C) δ 91.0 (s). HRMS (EI): m/z found 534.2716 ($[M]^+$), calcd for $C_{26}H_{48}FeN_4P_2$: 534.2704.

Preparation of 1,1′-Bis(dichlorophosphino)ferrocene (6). To a solution of 1,1′-bis[bis(diethylamino)phosphino]ferrocene (**5**) (172.0 mg, 0.322 mmol) in ether (3 mL) was added hydrogen chloride in ether solution (1.0 mol dm^{-3}, 2.60 mL, 2.60 mmol) at −78 °C. After the solution was warmed to room temperature for 4 h, the solvent was removed in vacuo. Benzene was added to the residue and the solution was filtered through Celite®. The solvent was removed to afford 1,1′-bis(dichlorophosphino)ferrocene (**6**) (105.0 mg, 0.271 mmol, 84%) as waxy orange solids. **6**: ^{1}H NMR (300 MHz, C_6D_6, 25 °C) δ 4.02 (br, 4H, C_5H_4), 4.19 (br, 4H, C_5H_4). ^{13}C{^{1}H} NMR (75 MHz, C_6D_6, 25 °C) δ 72.61 (d, $^2J_{PC}$ = 22.2 Hz, CH), 74.61 (br t, CH), 81.97 (d, $^1J_{PC}$ = 55.4 Hz, *ipso*-C_5H_4). ^{31}P NMR (120 MHz, C_6D_6, 25 °C) δ 162.4 (s). HRMS (EI): m/z found 385.8219 ($[M]^+$), calcd for $C_{10}H_8{}^{35}Cl_4FeP_2$: 385.8206.

Synthesis and Isolation of 1,1′-Bis[(*E*)-diphosphenyl]ferrocene ((*E*,*E*)-1a). In a glovebox filled with argon, butyllithium in hexane (1.50 mol dm^{-3}, 302 µL, 0.453 mmol) was added to an ether solution (5 mL) of H_2PTbt (**4a**) (265.0 mg, 0.453 mmol) at −40 °C. The solution of LiP(H)Tbt (**7a**) obtained here was warmed to room temperature for 30 min and cooled to −40 °C. The solution was added to a solution of 1,1′-bis(dichlorophosphino)ferrocene (**6**) (87.8 mg, 0.226 mmol) in benzene (30 mL) at room temperature. After the reaction mixture was stirred for 4 h at room temperature, DBU (67.6 µL, 0.453 mmol) was added to the reaction mixture at room temperature. After removal of the solvents, hexane was added to the residue and the reaction mixture was filtered through Celite®. The filtrate was cooled to −40 °C, the suspension was filtered through a glass filter to afford (*E*,*E*)-**1a** (217.2 mg, 0.154 mmol, 68%) as purple crystals. (*E*,*E*)-**1a**: mp 265–266 °C. ^{1}H NMR (300 MHz, C_6D_6, 25 °C) δ 0.21 (s, 36H, Si(CH_3)$_3$), 0.27 (br, 72H, Si(CH_3)$_3$), 1.55 (s, 2H, CH), 2.38 (br, 2H, CH), 2.57 (br, 2H, CH), 4.58 (A_2B_2, $^1J_{HH}$ = 1.8 Hz, 4H, C_5H_4), 4.96 (A_2B_2, $^1J_{HH}$ = 1.8 Hz, 4H, C_5H_4), 6.71 (br, 2H, C_6H_2), 6.80 (br, 2H, C_6H_2). ^{31}P NMR (120 MHz, C_6D_6, 25 °C) δ 488.9, 497.3 (ABq, $^1J_{PP}$ = 550 Hz). UV–vis (benzene): λ_{max} 384 (ε 7300), 480 (sh, ε 1800), 539 (ε 2200) nm. HRMS (FAB): m/z found 1411.5419 ($[M + H]^+$), calcd for $C_{64}H_{127}FeP_4Si_{12}$: 1411.5409. Anal. Calcd for $C_{64}H_{126}FeP_4Si_{12}$: C, 54.42; H, 8.99%. Found: C, 54.30; H, 9.01%. Satisfactory ^{13}C NMR data of (*E*,*E*)-**1a** could not be obtained due to its low solubility in common organic solvents.

Synthesis and Isolation of 1,1′-Bis[(*E*)-diphosphenyl]ferrocene ((*E*,*E*)-1b). In a glovebox filled with argon, butyllithium in hexane (1.50 mol dm^{-3}, 285 µL, 0.428 mmol) was added to an ether solution (5 mL) of H_2PBbt (**4b**) (281.3 mg, 0.428 mmol) at −40 °C. The solution of LiP(H)Bbt (**7b**) obtained here was warmed to room temperature for 1 h and cooled to −40 °C. The solution was added to a solution of 1,1′-bis(dichlorophosphino)-ferrocene (**6**) (83.0 mg, 0.214 mmol) in benzene (30 mL) at room temperature. After the reaction mixture was stirred for 4 h at room temperature, DBU (65.0 µL, 0.428 mmol) was added to the reaction mixture at room temperature. After removal of the solvents, benzene and hexane was added to the residue and the reaction mixture was filtered through Celite®. The filtrate was cooled to −40 °C, the suspension was filtered through a glass filter to afford (*E*,*E*)-**1b** (206.6 mg, 0.133 mmol, 62%) as purple crystals. (*E*,*E*)-**1b**: mp 278–280 °C. ^{1}H NMR (300 MHz, C_6D_6, 25 °C) δ 0.29 (s, 72H, Si(CH_3)$_3$), 0.41 (s, 54H, Si(CH_3)$_3$), 2.73 (s, 4H, CH), 4.58 (A_2B_2, $^1J_{HH}$ = 1.8 Hz, 4H, C_5H_4), 4.93 (A_2B_2, $^1J_{HH}$ = 1.8 Hz, 4H, C_5H_4), 7.11 (s, 4H, C_6H_2). ^{13}C{^{1}H} NMR (75 MHz, C_6D_6, 50 °C) δ 1.91 (s, CH_3), 5.65 (s, CH_3), 22.53 (s, *C*(SiMe$_3$)$_3$), 33.23 (s, *C*H(SiMe$_3$)$_2$ × 2), 73.64 (br, C_5H_4), 75.07 (s, C_5H_4), 86.30 (d, $^1J_{PC}$ = 48.7 Hz, *ipso*-C_5H_4), 127.42 (br, *m*-C_6H_2), 135.38 (d, $^1J_{PC}$ = 30.8 Hz, *ipso*-C_6H_2), 146.18 (s, C_6H_2), 146.49 (br, C_6H_2). ^{31}P NMR (120 MHz, C_6D_6, 25 °C) δ 491.1, 496.9 (ABq, $^1J_{PP}$ = 550 Hz). UV–vis (benzene): λ_{max} 389 (ε 7400), 485 (sh, ε 1300), 553 (ε 2200) nm. HRMS (FAB): m/z found 1556.6230 ($[M]^+$), calcd for $C_{70}H_{142}FeP_4Si_{14}$: 1556.6278. Anal. Calcd for $C_{70}H_{142}FeP_4Si_{14}$: C, 54.00; H, 9.19%. Found: C, 53.89; H, 9.37%.

Reaction of 1,1′-Bis[(*E*)-diphosphenyl]ferrocene ((*E*,*E*)-1a) with Methanol. In a glovebox filled with argon, 1,1′-bis[(*E*)-diphosphenyl]ferrocene ((*E*,*E*)-**1a**) (210.6 mg, 0.149 mmol) was dissolved in benzene-d_6 (0.8 mL), and the solution was placed in an NMR tube. After methanol (38 mL, 1.5 mmol) was added to the solution at room temperature, the tube was degassed and sealed. Upon standing at room temperature for 24 h, the color of the solution changed from purple to orange. The tube was opened, and the solvent was evaporated. Separation of the reaction mixture by PTLC using hexane and CH_2Cl_2 as eluents gave H_2PTbt (**4a**) (172.7 mg, 0.295 mmol, 99%) and [Fe{C_5H_4PH(O)OMe}$_2$] (**9**) (45.9 mg, 0.134 mmol, 90%), respectively. **9**: orange solid. mp 177–179 °C. ^{1}H NMR (300 MHz, C_6D_6, 25 °C) δ 3.35 (d, $^3J_{PH}$ = 11.9 Hz, 3H, $POCH_3$), 4.30–4.73 (m, 4H, C_5H_4), 7.49 (d, $^1J_{PH}$ = 561 Hz, 1H, PH). ^{13}C{^{1}H} NMR (75 MHz, C_6D_6, 25 °C) δ 51.76 (m, $POCH_3$), 69.95 (d, J_{PC} = 16.1 Hz, *ipso*-C_5H_4), 72.22 (d, J_{PC} = 15.7 Hz, C_5H_4), 73.56 (m, C_5H_4). ^{31}P NMR (120 MHz, C_6D_6, 25 °C) δ 29.3 (brd, $^1J_{HP}$ = 561 Hz). HRMS (EI): m/z found 341.9883 ($[M]^+$), calcd for $C_{12}H_{16}FeO_4P_2$: 341.9873. Anal. Calcd for $C_{12}H_{16}FeO_4P_2$: C, 42.14; H, 4.71%. Found: C, 42.48; H, 4.79%.

Reaction of 1,1′-Bis[(*E*)-diphosphenyl]ferrocene ((*E*,*E*)-1b) with Chromium Pentacarbonyl Acetonitrile Complex. In a glovebox filled with argon, 1,1′-bis[(*E*)-diphosphenyl]ferrocene ((*E*,*E*)-**1b**) (30.0 mg, 19.3 µmol) and [Cr(CO)$_5$(CH_3CN)] (50.0 mg, 215 µmol) in benzene-d_6 (0.8 mL) was placed in an NMR tube. After three freeze–pump–thaw cycles, the NMR tube was evacuated and sealed. After heating the tube at 50 °C for 2 h, the signals for (*E*,*E*)-**1b** disappeared in the ^{31}P NMR spectrum. The tube was opened, and the insoluble materials were removed by filtering through Celite®. After removal of the solvent, the reaction mixture was separated by GPLC to afford the chromium complex, (*Z*,*Z*)-**1b·Cr(CO)$_4$** (27.0 mg, 15.7 µmol; 81%). (*Z*,*Z*)-**1b·Cr(CO)$_4$**: purple crystals. mp 165 °C (dec.). ^{1}H NMR (400 MHz, C_6D_6, 20 °C) δ 0.21 (s, 36H, Si(CH_3)$_3$), 0.30 (s, 36H, Si(CH_3)$_3$), 0.32 (s, 54H, Si(CH_3)$_3$), 2.92 (s, 2H, CH), 2.93 (s, 2H, CH), 4.30 (A_2B_2, $^1J_{HH}$ = 1.8 Hz, 4H, C_5H_4), 4.69 (A_2B_2, $^1J_{HH}$ = 1.8 Hz, 4H, C_5H_4), 6.92 (brs, 4H, C_6H_2). ^{13}C{^{1}H} NMR (100 MHz, C_6D_6, 20 °C) δ 2.70 (s, Si(CH_3)$_3$), 5.48 (s, Si(CH_3)$_3$), 22.27 (s, *C*(SiMe$_3$)$_3$), 31.80 (brs, *C*H(SiMe$_3$)$_2$ × 2), 75.40 (s, β-C_5H_4), 78.60 (brs, α-C_5H_4), 87.66 (brd, J_{PC} = 28.8 Hz), 127.45 (br, *m*-C_6H_2), 137.23 (dd, J_{PC} = 58.0 and 10.7 Hz, *ipso*-C_6H_2), 146.29 (s, *p*-C_6H_2), 147.35 (br, *o*-C_6H_2), 216.91 (brd, J_{PC} = 39.1 Hz, CO), 219.24 (brt, CO). ^{31}P NMR (120 MHz, C_6D_6, 25 °C) δ 386.4, 295.9 (AA′BB′, $^1J_{PP}$ = ±620.1, $^2J_{PP}$ = ±37.3, $^3J_{PP}$ = ∓18.7, $|^4J_{PP}| < 4.0$ Hz). UV–vis (*n*-hexane): λ_{max} 360 (sh, ε 4400), 492 (ε 5400), 640 (sh, ε 1300) nm. IR (nujol): ν(CO) 2015, 1954, 1935, 1910 cm^{-1}. HRMS (FAB): m/z found 1721.5421 ($[M]^+$), calcd for $C_{74}H_{142}CrFeO_4P_4Si_{14}$: 1721.5401.

Reaction of 1,1′-Bis[(*E*)-diphosphenyl]ferrocene ((*E*,*E*)-1b) with Molybdenum Tetracarbonyl Norbornadiene Complex.

1,1′-Bis[(*E*)-diphosphenyl]ferrocene ((*E*,*E*)-**1b**) (32.0 mg, 20.6 μmol) and [Mo(CO)$_4$(nbd)] (57.0 mg, 206 μmol) in benzene-d_6 (0.8 mL) was placed in an NMR tube. After three freeze–pump–thaw cycles, the NMR tube was evacuated and sealed. When the NMR tube was heated at 50 °C for 2 h, the signals for (*E*,*E*)-**1b** disappeared in the ^{31}P NMR spectrum. The tube was opened, and the insoluble materials were removed by filtering through Celite®. After removal of the solvent, the reaction mixture was separated by GPLC to afford the molybdenum complex, (*Z*,*Z*)-**1b·Mo(CO)$_4$** (27.0 mg, 15.3 μmol; 74%). (*Z*,*Z*)-**1b·Mo(CO)$_4$**: purple crystals. mp 132 °C (dec.). ^{1}H NMR (300 MHz, C_6D_6, 25 °C) δ 0.21 (s, 36H, Si(CH$_3$)$_3$), 0.29 (s, 36H, Si(CH$_3$)$_3$), 0.32 (s, 54H, Si(CH$_3$)$_3$), 2.87 (s, 2H, CH), 2.90 (s, 2H, CH), 4.32 (A$_2$B$_2$, $^1J_{HH}$ = 1.8 Hz, 4H, C_5H_4), 4.62 (A$_2$B$_2$, $^1J_{HH}$ = 1.8 Hz, 4H, C_5H_4), 6.92 (brs, 4H, C_6H_2). ^{13}C{^{1}H} NMR (75 MHz, C_6D_6, 23 °C) δ 2.55 (s, Si(CH$_3$)$_3$), 5.34 (s, Si(CH$_3$)$_3$), 22.11 (s, *C*(SiMe$_3$)$_3$), 31.77 (brs, *C*H(SiMe$_3$)$_2$), 31.84 (brs, *C*H(SiMe$_3$)$_2$), 75.02 (s, β-C_5H_4), 78.69 (brd, J_{PC} = 6.1 Hz, α-C_5H_4), 87.42 (m, *ipso*-C_5H_4), 127.62 (br, *m*-C_6H_2), 137.13 (m, *ipso*-C_6H_2), 146.21 (s, *p*-C_6H_2), 147.05 (br, *o*-C_6H_2), 214.85 (m, CO), 223.14 (br, CO). ^{31}P NMR (120 MHz, C_6D_6, 25 °C) δ 358.7, 304.3 (AA′BB′, $^1J_{PP}$ = ±606.7, $^2J_{PP}$ = ±29.7, $^3J_{PP}$ = ∓14.9, $|^4J_{PP}| < 4.0$ Hz). UV–vis (*n*-hexane): λ_{max} 362 (sh, ε 5400), 488 (ε 4100), 627 (sh, ε 640) nm. IR (nujol): ν(CO) 2028, 1958, 1942, 1906 cm^{-1}. HRMS (FAB): *m*/*z* found 1764.5075 ([M]$^+$), calcd for $C_{74}H_{142}Fe^{98}MoO_4P_4Si_{14}$: 1764.5046.

Reaction of 1,1′-Bis[(*E*)-diphosphenyl]ferrocene ((*E*,*E*)-1b) with Molybdenum Pentacarbonyl Acetonitrile Complex. 1,1′-Bis[(*E*)-diphosphenyl]ferrocene ((*E*,*E*)-**1b**) (23.1 mg, 14.8 μmol) and [Mo(CO)$_5$(CH$_3$CN)] (40.8 mg, 148 μmol) in benzene-d_6 (0.7 mL) was placed in an NMR tube. After three freeze–pump–thaw cycles, the NMR tube was evacuated and sealed. After heating of the tube at 50 °C for 3 h, the signals for (*E*,*E*)-**1b** disappeared in the ^{31}P NMR spectrum. The tube was opened, and the insoluble materials were removed by filtering through Celite®. After removal of the solvent, the reaction mixture was separated by GPLC to afford (*Z*,*Z*)-**1b·Mo(CO)$_4$** (18.2 mg, 10.3 μmol; 70%).

Reaction of 1,1′-Bis[(*E*)-diphosphenyl]ferrocene ((*E*,*E*)-1b) with Tungsten Tetracarbonyl 1,5-Cyclooctadiene Complex. 1,1′-Bis[(*E*)-diphosphenyl]ferrocene ((*E*,*E*)-**1b**) (48.0 mg, 31.0 μmol) and [W(CO)$_4$(cod)] (125.1 mg, 310 μmol) in benzene-d_6 (0.7 mL) was placed in an NMR tube. After three freeze–pump–thaw cycles, the NMR tube was evacuated and sealed. When the NMR tube was heated at 50 °C for 3 h, the signals for (*E*,*E*)-**1b** disappeared in the ^{31}P NMR spectrum. The tube was opened, and the insoluble materials were removed by filtering through Celite®. After removal of the solvent, the reaction mixture was separated by GPLC to afford the tungsten complex, (*Z*,*Z*)-**1b·W(CO)$_4$** (51.2 mg, 27.6 μmol; 89%). (*Z*,*Z*)-**1b·W(CO)$_4$**: dark red crystals. mp 144 °C (dec.). ^{1}H NMR (400 MHz, C_6D_6, 24 °C) δ 0.20 (s, 36H, Si(CH$_3$)$_3$), 0.29 (s, 36H, Si(CH$_3$)$_3$), 0.32 (s, 54H, Si(CH$_3$)$_3$), 2.90 (s, 2H, CH), 2.91 (s, 2H, CH), 4.32 (A$_2$B$_2$, $^1J_{HH}$ = 1.8 Hz, 4H, C_5H_4), 4.62 (A$_2$B$_2$, $^1J_{HH}$ = 1.8 Hz, 4H, C_5H_4), 6.92 (brs, 4H, C_6H_2). ^{13}C{^{1}H} NMR (100 MHz, C_6D_6, 20 °C) δ 2.57 (s, Si(CH$_3$)$_3$), 5.37 (s, Si(CH$_3$)$_3$), 22.17 (s, *C*(SiMe$_3$)$_3$), 31.82 (s, *C*H(SiMe$_3$)$_2$), 31.89 (s, *C*H(SiMe$_3$)$_2$), 75.11 (s, β-C_5H_4), 78.90 (brd, J_{PC} = 6.2 Hz, α-C_5H_4), 87.80 (m, *ipso*-C_5H_4), 127.75 (br, *m*-C_6H_2), 137.74 (dd, J_{PC} = 12.3, 60.5 Hz, *ipso*-C_6H_2), 146.29 (s, *p*-C_6H_2), 147.15 (brs, *o*-C_6H_2), 199.08 (brt, CO), 205.19 (brd, J = 33.2 Hz, CO). ^{31}P NMR (120 MHz, C_6D_6, 24 °C) δ 307.2 (the satellite signals of $^1J_{WP}$ = 245.1 Hz), 283.7 (AA′BB′, $^1J_{PP}$ = ±604.6 Hz, $^2J_{PP}$ = ±29.0, $^3J_{PP}$ = ∓14.5, $|^4J_{PP}| < 4.0$ Hz). UV–vis (*n*-hexane): λ_{max} 363 (sh, ε 4400), 492 (ε 5700), 620 (sh, ε 1500) nm. IR (nujol): ν(CO) 2024, 1951, 1932, 1896 cm^{-1}. LRMS (FAB): *m*/*z* found 1852 ([M + H]$^+$), calcd for $C_{74}H_{143}FeO_4P_4Si_{14}W$: 1852. Anal. Calcd for $C_{74}H_{142}FeO_4P_4Si_{14}W$: C, 47.97; H, 7.73%. Found: C, 47.57; H, 7.51%.

Reaction of 1,1′-Bis[(*E*)-diphosphenyl]ferrocene ((*E*,*E*)-1b) with Tungsten Pentacarbonyl Acetonitrile Complex. 1,1′-Bis[(*E*)-diphosphenyl]ferrocene ((*E*,*E*)-**1b**) (31.1 mg, 20.0 μmol) and [W(CO)$_5$(CH$_3$CN)] (73.0 mg, 200 μmol) in benzene-d_6 (0.8 mL) was placed in an NMR tube. After three freeze–pump–thaw cycles, the NMR tube was evacuated and sealed. The solution was heated at 50 °C for 2.5 h, during which time the original purple color changed to dark red, and the signals for (*E*,*E*)-**1b** disappeared in the ^{31}P NMR spectrum. The tube was opened, and the insoluble materials were removed by filtering through Celite®. After removal of the solvent, the reaction mixture was separated by GPLC to afford (*Z*,*Z*)-**1b·W(CO)$_4$** (35.3 mg, 19.1 μmol; 96%).

Theoretical Calculations. All theoretical calculations were carried out using the Gaussian 98 program[35] with density function theory at the B3LYP method. The geometries of (*E*,*E*)-**8a**, (*E*,*E*)-**8b**, and (*Z*,*Z*)-**14** were optimized by using the 6-31G(d) basis sets. It was confirmed that the optimized structures of (*E*,*E*)-**8a**, (*E*,*E*)-**8b**, and (*Z*,*Z*)-**14** have minimum energies by frequency calculations. The TDDFT calculations of (*E*,*E*)-**8a**, (*E*,*E*)-**8b**, and (*Z*,*Z*)-**14** were performed at TZ(2d) for Fe, 6-311+G(2d) for P, and 6-31G(d) for C and H (for (*E*,*E*)-**8a** and (*E*,*E*)-**8b**) or 6-31G(d) (for (*Z*,*Z*)-**14**) basis sets. Theoretically optimized coordinations of (*E*,*E*)-**8a**, (*E*,*E*)-**8b**, and (*Z*,*Z*)-**14** are shown in Table S1, S2, and S4, respectively.

X-ray Crystallographic Analyses of (*E*,*E*)-1a, (*E*,*E*)-1b, and (*Z*,*Z*)-1b·W(CO)$_4$. Single crystals of (*E*,*E*)-**1a**, (*E*,*E*)-**1b**, and (*Z*,*Z*)-**1b·W(CO)$_4$** were obtained by slow recrystallization from benzene solution at room temperature in a degassed and sealed tube (for (*E*,*E*)-**1a** and (*E*,*E*)-**1b**) or in a glovebox filled with argon (for (*Z*,*Z*)-**1b·W(CO)$_4$**). The intensity data were collected on a Rigaku Mercury CCD diffractometer with graphite-monochromated Mo Kα radiation (λ = 0.71070 Å) (for (*E*,*E*)-**1a** and (*E*,*E*)-**1b**) or on a Rigaku Saturn70 CCD system with VariMax Mo Optic using Mo Kα radiation (λ = 0.71070 Å) (for (*Z*,*Z*)-**1b·W(CO)$_4$**). Selected structural parameters and crystal data of (*E*,*E*)-**1a**, (*E*,*E*)-**1a**, and (*Z*,*Z*)-**1b·W(CO)$_4$** are shown in Tables 3, 12, and 13, respectively. The structure was solved by direct method (SHELXS-97)[36] and refined by full-matrix least-squares procedures on F^2 for all reflections (SHELXL-97).[37] All non-hydrogen atoms were refined anisotropically. All hydrogen atoms were placed using AFIX instructions. All atoms of (*E*,*E*)-**1a** except for the benzene ring of the Tbt group were disordered and their occupancies were refined (0.62:0.38). The cyclopentadienyl ring and phosphorus atoms of (*E*,*E*)-**1b** were disordered, and their occupancies were refined (0.89:0.11). The cyclopentadienyl ring of the minor part of the disordered carbon atoms of (*E*,*E*)-**1b** are restrained using SADI instructions and refined isotropically. One of the CH(SiMe$_3$)$_2$ groups at the *ortho*-position and the C(SiMe$_3$)$_3$ group at the *para*-position of the Bbt group of (*E*,*E*)-**1b** were disordered, and the occupancies were refined (0.57:0.43). One of the CH(SiMe$_3$)$_2$ groups at the *ortho*-position and two C(SiMe$_3$)$_3$ groups at the *para*-position of the Bbt group of (*Z*,*Z*)-**1b·W(CO)$_4$** were disordered, and the occupancies were refined (The final ratios were 0.52:0.48, 0.56:0.44, and 0.73:0.27). Crystallographic data reported in this manuscript have been deposited with Cambridge Crystallographic Data Centre as supplementary publication Nos. CCDC-287252 ((*E*,*E*)-**1a**), 287251 ((*E*,*E*)-**1a**), and 617389

Table 13. Crystallographic Data and Experimental Parameters for the Crystal Structure Analyses of (*E*,*E*)-**1a**, (*E*,*E*)-**1b**, and (*Z*,*Z*)-**1b**·**W(CO)$_4$**

	(*E*,*E*)-**1a**	(*E*,*E*)-**1b**	(*Z*,*Z*)-**1b**·**W(CO)$_4$**
Formula	$C_{64}H_{126}FeP_4Si_{12}$	$C_{70}H_{142}FeP_4Si_{14}$	$C_{74}H_{142}FeO_4P_4Si_{14}W$
Formula weight	1412.46	1556.83	1852.72
Crystal dimensions/mm^3	0.30 × 0.20 × 0.10	0.40 × 0.30 × 0.15	0.15 × 0.10 × 0.05
Collection temperature/K	103(2)	103(2)	103(2)
Crystal system	triclinic	monoclinic	triclinic
Space group	$P\bar{1}$ (#2)	$C2/c$ (#15)	$P\bar{1}$ (#2)
a/Å	10.834(3)	22.9804(5)	9.9493(8)
b/Å	10.640(3)	11.6477(3)	12.7337(11)
c/Å	19.972(6)	34.7151(8)	42.806(5)
α/°	75.001(10)	90	97.960(4)
β/°	87.417(12)	96.8190(9)	91.607(4)
γ/°	71.851(9)	90	112.083(8)
Volume/Å^3	2111.7(11)	9226.4(4)	4957.9(8)
Z	1	4	2
Density/g cm^{-3}	1.111	1.121	1.241
Independent reflections	7272	8118	17117
No. of parameters	668	510	1005
R_1 [$I > 2\sigma(I)$]	0.0780	0.0765	0.1063
wR_2 [$I > 2\sigma(I)$]	0.1619	0.2095	0.2446
R_1 (all data)	0.1298	0.0995	0.1855
wR_2 (all data)	0.1963	0.2281	0.2957
Goodness of fit	1.096	1.049	1.138

((*Z*,*Z*)-**1b**·**W(CO)$_4$**). Copies of the data can be obtained free of charge via www.ccdc.cam.ac.uk/conts/retrieving.html (or from the Cambridge Crystallographic Data Centre, 12, Union Road, Cambridge, CB2 1EZ, UK; fax: +44 1223 336033; or deposit@ccdc.cam.ac.uk).

This work was supported in part by Grants-in-Aid for Creative Scientific Research (No. 17GS0207), Scientific Research (No. 18750030), and the 21st Century COE, Kyoto University Alliance for Chemistry from the Ministry of Education, Culture, Sports, Science and Technology, Japan. N. N. thanks for the general support from the Kyoto Sustainability Initiative and the Institute of Sustainability Science, Kyoto University.

Supporting Information

Tables S1–S6 are in PDF format. This material is available free of charge on the web at http://www.csj.jp/journals/bcsj/.

References

Dedicated to the memory of the late Prof. Yoshihiko Ito.

1 a) L. Weber, *Chem. Rev.* **1992**, *92*, 1839. b) P. P. Power, *Chem. Rev.* **1999**, *99*, 3463. c) N. Tokitoh, *J. Organomet. Chem.* **2000**, *611*, 217. d) B. Twamley, P. P. Power, *Chem. Commun.* **1998**, 1979. e) B. Twamley, C. D. Sofield, M. M. Olmstead, P. P. Power, *J. Am. Chem. Soc.* **1999**, *121*, 3357.

2 M. Yoshifuji, I. Shima, N. Inamoto, K. Hirotsu, T. Higuchi, *J. Am. Chem. Soc.* **1981**, *103*, 4587.

3 a) B. Çetinkaya, A. Hudson, M. F. Lappert, H. Goldwhite, *J. Chem. Soc., Chem. Commun.* **1982**, 609. b) B. Çetinkaya, P. B. Hitchcock, M. L. Lappert, A. J. Thorne, H. Goldwhite, *J. Chem. Soc., Chem. Commun.* **1982**, 691. c) A. J. Bard, A. H. Cowley, J. E. Kilduff, J. K. Leland, N. C. Norman, M. Pakulski, G. A. Heath, *J. Chem. Soc., Dalton Trans.* **1987**, 249. d) M. Culcasi, G. Gronchi, J. Escudié, C. Couret, L. Pujol, P. Tordo, *J. Am. Chem. Soc.* **1986**, *108*, 3130. e) S. Shah, S. C. Burdette, S. Swavey, F. L. Urbach, J. D. Protasiewicz, *Organometallics* **1997**, *16*, 3395.

4 a) N. Tokitoh, Y. Arai, R. Okazaki, S. Nagase, *Science* **1997**, *277*, 78. b) N. Tokitoh, Y. Arai, T. Sasamori, R. Okazaki, S. Nagase, H. Uekusa, Y. Ohashi, *J. Am. Chem. Soc.* **1998**, *120*, 433. c) T. Sasamori, N. Takeda, N. Tokitoh, *Chem. Commun.* **2000**, 1353. d) T. Sasamori, Y. Arai, N. Takeda, R. Okazaki, Y. Furukawa, M. Kimura, S. Nagase, N. Tokitoh, *Bull. Chem. Soc. Jpn.* **2002**, *75*, 661. e) T. Sasamori, N. Takeda, M. Fujio, M. Kimura, S. Nagase, N. Tokitoh, *Angew. Chem., Int. Ed.* **2002**, *41*, 139. f) T. Sasamori, N. Takeda, N. Tokitoh, *J. Phys. Org. Chem.* **2003**, *16*, 450. g) T. Sasamori, E. Mieda, N. Takeda, N. Tokitoh, *Chem. Lett.* **2004**, *33*, 104. h) N. Nagahora, T. Sasamori, N. Takeda, N. Tokitoh, *Chem. Eur. J.* **2004**, *10*, 6146. i) T. Sasamori, E. Mieda, N. Nagahora, N. Takeda, N. Takagi, S. Nagase, N. Tokitoh, *Chem. Lett.* **2005**, *34*, 166. j) T. Sasamori, E. Mieda, N. Takeda, N. Tokitoh, *Angew. Chem., Int. Ed.* **2005**, *44*, 3717. k) T. Sasamori, E. Mieda, N. Nagahora, K. Sato, D. Shiomi, T. Takui, Y. Hosoi, Y. Furukawa, N. Takagi, S. Nagase, N. Tokitoh, *J. Am. Chem. Soc.* **2006**, *128*, 12582. l) T. Sasamori, A. Tsurusaki, N. Nagahora, K. Matsuda, Y. Kanemitsu, Y. Watanabe, Y. Furukawa, N. Tokitoh, *Chem. Lett.* **2006**, *35*, 1382.

5 M. Yoshifuji, *Bull. Chem. Soc. Jpn.* **1997**, *70*, 2881.

6 R. Pietschnig, E. Niecke, *Organometallics* **1996**, *15*, 891.

7 a) S. Shah, T. Concolio, A. L. Rheingold, J. D. Protasiewicz, *Inorg. Chem.* **2000**, *39*, 3860. b) C. Dutan, S. Shah, R. C. Smith, S. Choua, T. Berclaz, M. Geoffroy, J. D. Protasiewicz, *Inorg. Chem.* **2003**, *42*, 6241. c) R. C. Smith, J. D. Protasiewicz, *Eur. J. Inorg. Chem.* **2004**, 998.

8 a) N. Nagahora, T. Sasamori, N. Tokitoh, The 85th Annual Meeting of the Chemical Society of Japan, Yokohama, Japan, March 26–29, **2005**, Abstr. No. 1-B6-26. b) N. Tokitoh, E. Mieda, N. Nagahora, T. Sasamori, N. Takeda, N. Takagi, S. Nagase, Pacifichem 2005, Honolulu, Hawaii, December 15–20, **2005**,

Abstr. No. 1270. c) N. Nagahora, T. Sasamori, N. Tokitoh, *Chem. Lett.* **2006**, *35*, 220.

9 C. Moser, M. Nieger, R. Pietschnig, *Organometallics* **2006**, *25*, 2667.

10 a) F. Hartl, T. Mahabiersing, P. L. Floch, F. Mathey, L. Ricard, P. Rosa, S. Záliš, *Inorg. Chem.* **2003**, *42*, 4442. b) P. Rosa, N. Mézailles, L. Ricard, F. Mathey, P. L. Floch, Y. Jean, *Angew. Chem., Int. Ed.* **2001**, *40*, 1251. c) N. Mézailles, P. Rosa, L. Ricard, F. Mathey, P. L. Floch, *Organometallics* **2000**, *19*, 2941. d) P. Rosa, L. Ricard, P. L. Floch, F. Mathey, G. Sini, O. Eisenstein, *Inorg. Chem.* **1998**, *37*, 3154. e) P. L. Floch, D. Carmicheal, L. Ricard, F. Mathey, *Organometallics* **1992**, *11*, 2475. f) P. L. Floch, D. Carmicheal, L. Ricard, F. Mathey, *J. Am. Chem. Soc.* **1991**, *113*, 667.

11 a) S. Kawasaki, A. Nakamura, K. Toyota, M. Yoshifuji, *Organometallics* **2005**, *24*, 2983. b) F. Ozawa, S. Kawagishi, T. Ishiyama, M. Yoshifuji, *Organometallics* **2004**, *23*, 1325. c) T. Minami, H. Okamoto, S. Ikeda, R. Tanaka, F. Ozawa, M. Yoshifuji, *Angew. Chem., Int. Ed.* **2001**, *40*, 4501. d) M. Yoshifuji, Y. Ichikawa, N. Yamada, K. Toyota, *Chem. Commun.* **1998**, 27. e) M. Yoshifuji, Y. Ichikawa, K. Toyota, *Tetrahedron Lett.* **1997**, *38*, 1585. f) M. Yoshifuji, Y. Ichikawa, K. Toyota, E. Kasashima, Y. Okamoto, *Chem. Lett.* **1997**, 87.

12 When using ether or THF as a solvent for the reaction of 1,1′-bis(dichlorophosphino)ferrocene with LiP(H)Ar (Ar = Tbt or Bbt), the yields of (*E*,*E*)-**1a** and (*E*,*E*)-**1b** dramatically decreased.

13 M. Yoshifuji, N. Shinohara, K. Toyota, *Tetrahedron Lett.* **1996**, *37*, 7815.

14 M. Baudler, K. Glinka, *Chem. Rev.* **1993**, *93*, 1623, and references cited therein.

15 H. Hamaguchi, M. Tasumi, M. Yoshifuji, N. Inamoto, *J. Am. Chem. Soc.* **1984**, *106*, 508.

16 K. Hassler, F. Hofler, *Z. Anorg. Allg. Chem.* **1978**, *443*, 125.

17 D. E. Richardson, H. Taube, *Inorg. Chem.* **1981**, *20*, 1278.

18 a) L. N. Mulay, A. Attalla, *J. Am. Chem. Soc.* **1963**, *85*, 702. b) R. K. Bohn, A. Haaland, *J. Organomet. Chem.* **1966**, *5*, 470. c) M. K. Makova, E. V. Leonova, Y. S. Karimov, N. S. Kochetkova, *J. Organomet. Chem.* **1973**, *55*, 185.

19 a) M. Yoshifuji, T. Hashida, N. Inamoto, K. Hirotsu, T. Horiuchi, T. Higuchi, K. Ito, S. Nagase, *Angew. Chem., Int. Ed. Engl.* **1985**, *24*, 211. b) M. Yoshifuji, K. Shibayama, T. Hashida, K. Toyota, T. Niitsu, I. Matsuda, T. Sato, N. Inamoto, *J. Organomet. Chem.* **1986**, *311*, C63. c) P. Jutzi, U. Meyer, S. Opiela, B. Neumann, H.-G. Stanmmler, *J. Organomet. Chem.* **1992**, *439*, 279.

20 a) N. Iranpoor, B. L. Shaw, *Inorg. Chim. Acta* **1993**, *204*, 39. b) E. H. Wong, F. C. Bradley, *J. Organomet. Chem.* **1983**, *244*, 235. c) L.-C. Song, J.-T. Liu, Q.-M. Hu, G.-F. Wang, P. Zanello, M. Fontani, *Organometallics* **2000**, *19*, 5342. d) D. J. Brauer, C. Like, O. Stelzer, *J. Organomet. Chem.* **2001**, *626*, 106.

21 For selected $\lambda^3\sigma^3$-phosphines, see: a) M. Guerro, T. Roisnel, P. Pellon, D. Lorcy, *Inorg. Chem.* **2005**, *44*, 3347. b) R. Broussier, S. Ninoreille, C. Bourdon, O. Blacque, C. Ninoreille, M. Kubucki, B. Gautheron, *J. Organomet. Chem.* **1998**, *561*, 85. c) M. S. Balakrishna, T. K. Prakasha, S. S. Krishnamurthy, *J. Organomet. Chem.* **1990**, *390*, 203.

22 For $\lambda^3\sigma^2$-phosphaalkenes, see: a) S. Ito, K. Nishide, M. Yoshifuji, *Organometallics* **2006**, *25*, 1424. b) S. Ito, M. Yoshifuji, *Chem. Commun.* **2001**, 1208. c) H. Liang, K. Nishide, S. Ito, M. Yoshifuji, *Tetrahedron Lett.* **2003**, *44*, 8297.

23 For $\lambda^3\sigma^2$-diphosphenes, see: a) S. Ito, K. Nishide, M. Yoshifuji, *Tetrahedron Lett.* **2002**, *43*, 5075. b) D.-L. An, K. Toyota, M. Yasunami, M. Yoshifuji, *J. Organomet. Chem.* **1996**, *508*, 7.

24 I. E. Nifant'ev, A. A. Boricenko, L. F. Manzhukova, E. E. Nifant'ev, *Phosphorus, Sulfur, Silicon* **1992**, *68*, 99.

25 W. Strohmeier, G. Schönauer, *Chem. Ber.* **1961**, *94*, 1346.

26 M. A. M. Forgeron, M. Gee, R. E. Wasylishen, *J. Phys. Chem. A* **2004**, *108*, 4895.

27 N. Nagahora, T. Sasamori, N. Tokitoh, unpublished results.

28 M. Zhou, C. W. Bauschlicher, *Chem. Rev.* **2001**, *101*, 1931.

29 a) B. R. Kimpton, W. McFarlane, A. S. Muir, P. G. Patel, J. L. Bookham, *Polyhedron* **1993**, *12*, 2525. b) P. M. Hodges, S. A. Jackson, J. Jacke, M. Poliakoff, J. J. Turner, F.-W. Grevels, *J. Am. Chem. Soc.* **1990**, *112*, 1234. c) M. Y. Darensbourg, N. Walker, R. B. Robert, *Inorg. Chem.* **1978**, *17*, 52. d) G. R. Dobson, R. A. Brown, *J. Inorg. Nucl. Chem.* **1972**, *34*, 2785.

30 J. Chatt, H. R. Watson, *J. Chem. Soc.* **1961**, 4980.

31 A. B. Pangborn, M. A. Giardello, R. H. Grubbs, R. K. Rosen, F. J. Timmers, *Organometallics* **1996**, *15*, 1518.

32 T.-Y. Dong, L.-L. Lai, *J. Organomet. Chem.* **1996**, *509*, 131.

33 D. J. Dellinger, D. M. Sheehan, N. K. Christensen, J. G. Lindberg, M. H. Caruthers, *J. Am. Chem. Soc.* **2003**, *125*, 940.

34 G. R. Dobson, M. F. Sayed, I. W. Stolz, R. K. Sheline, *Inorg. Chem.* **1962**, *1*, 526.

35 M. J. Frisch, G. W. Trucks, H. B. Schlegel, G. E. Scuseria, M. A. Robb, J. R. Cheeseman, J. A. Montgomery, Jr., T. Vreven, K. N. Kudin, J. C. Burant, J. M. Millam, S. S. Iyengar, J. Tomasi, V. Barone, B. Mennucci, M. Cossi, G. Scalmani, N. Rega, G. A. Petersson, H. Nakatsuji, M. Hada, M. Ehara, K. Toyota, R. Fukuda, J. Hasegawa, M. Ishida, T. Nakajima, Y. Honda, O. Kitao, H. Nakai, M. Klene, X. Li, J. E. Knox, H. P. Hratchian, J. B. Cross, C. Adamo, J. Jaramillo, R. Gomperts, R. E. Stratmann, O. Yazyev, A. J. Austin, R. Cammi, C. Pomelli, J. W. Ochterski, P. Y. Ayala, K. Morokuma, G. A. Voth, P. Salvador, J. J. Dannenberg, V. G. Zakrzewski, S. Dapprich, A. D. Daniels, M. C. Strain, O. Farkas, D. K. Malick, A. D. Rabuck, K. Raghavachari, J. B. Foresman, J. V. Ortiz, Q. Cui, A. G. Baboul, S. Clifford, J. Cioslowski, B. B. Stefanov, G. Liu, A. Liashenko, P. Piskorz, I. Komaromi, R. L. Martin, D. J. Fox, T. Keith, M. A. Al-Laham, C. Y. Peng, A. Nanayakkara, M. Challacombe, P. M. W. Gill, B. Johnson, W. Chen, M. W. Wong, C. Gonzalez, J. A. Pople, *Gaussian 98, Revision C.02*, Gaussian, Inc., Wallingford CT, **2004**.

36 G. M. Sheldrick, *Acta Crystallogr., Sect. A* **1990**, *46*, 467.

37 G. M. Sheldrick, *SHELXL-97, Program for the Refinement of Crystal Structures*, University of Göttingen, Göttingen, **1997**.